ATLAS PUB Note

ATL-PHYS-PUB-2022-009

11th March 2022

Standard Model Summary Plots February 2022

The ATLAS Collaboration

This note presents cross section summary plots for ATLAS cross section measurements as of February 2022. Figures with references contain hyperlinks to ATLAS publications and preliminary documentation.

Contents

1 Introduction

This document summarizes the Standard Model summary plots with the inputs available at 23/02/2022. The scripts for the creation of these plots are available at [1].

2 Updates since July 2021

Since the last publication of these summary plots [2], the following results have been updated:

- WWW at 13 TeV: The cross-section measurements with full Run 2 dataset are published as a paper (previous results were presented as a conference note) [3].
- Total H at 13 TeV: The measured total Higgs boson production cross section is updated using the full Run 2 dataset [4].
- $H \to \tau\tau$ at 13 TeV: Fiducial cross sections measured using the full Run 2 dataset are submitted as a paper (previous results were presented as a conference note) [5].
- H: **VBF**, **ggF**, **VH** and $t\bar{t}$**H** at 13 TeV: Latest results for gluon–gluon fusion (ggF), vector-boson fusion (VBF) processes, and for associated production with vector bosons (VH) or top-quarks ($t\bar{t}$H) are available with a new combination of measurements of Higgs boson production cross sections and branching fractions [6].

Only Figures 1, 2, 3, 5, 6, 8, 9, 11, 14, 17, 18, 19, 20, 21 and 24 are affected by the aforementioned updates.

3 Total cross section overview plots

Figures 1 and 2 summarize several Standard Model total production cross-section measurements, corrected for branching fractions, compared to the corresponding theoretical expectations. The luminosity used for each measurement is indicated in the table. Some measurements have been extrapolated using branching ratios as predicted by the Standard Model for the Higgs boson. Uncertainties for the theoretical predictions are quoted from the original ATLAS papers. They were not always evaluated using the same prescriptions for PDFs and scales.

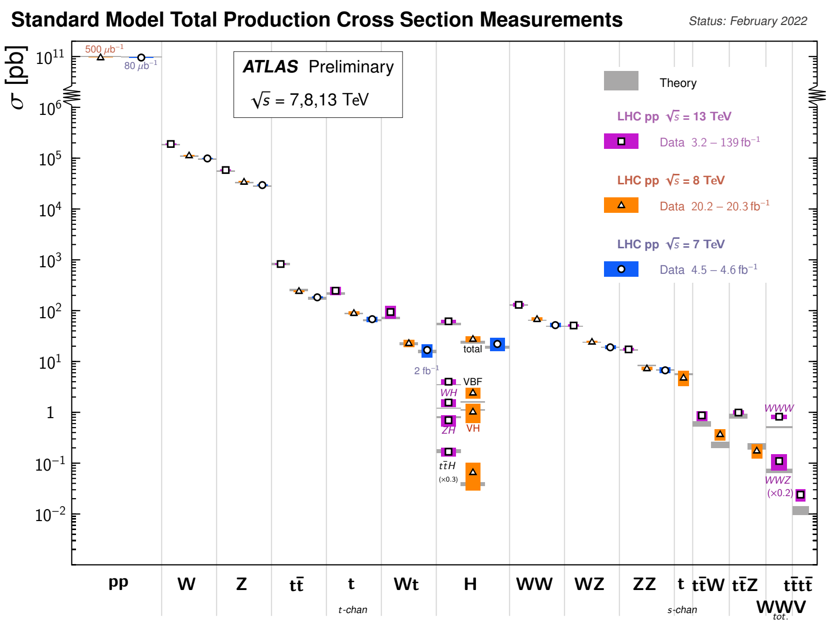

(a)

Standard Model Production Cross Section Measurements

Status: February 2022

ATLAS Preliminary

$\sqrt{s}$ = 5, 7, 8, 13 TeV

Model	E_{CM} [TeV]	$\int\mathcal{L}\,dt$[fb^{-1}]	Measurement	Theory	Reference
pp	8	50×10^{-8}	$\sigma = 96.07 \pm 0.18 \pm 0.91$ mb	$\sigma = 99.55 \pm 2.14$ mb (COMPETE HPR1R2)	PLB 761 (2016) 158
pp	7	8×10^{-8}	$\sigma = 95.35 \pm 0.38 \pm 1.3$ mb	$\sigma = 97.26 \pm 2.12$ mb (COMPETE HPR1R2)	Nucl. Phys. B, 486-548 (2014)
W	13	0.081	$\sigma = 190.1 \pm 0.2 \pm 6.4$ nb	$\sigma = 184.9 + 6 - 6.1$ nb (DYNNLO + CT14NNLO)	PLB 759 (2016) 601
W	8	20.2	$\sigma = 112.69 \pm 3.1$ nb	$\sigma = 110.919889503 \pm 3.7$ nb (DYNNLO + CT14NNLO)	EPJC 79 (2019) 760
W	7	4.6	$\sigma = 98.71 \pm 0.028 \pm 2.191$ nb	$\sigma = 95.9 \pm 2.9$ nb (DYNNLO + CT14NNLO)	EPJC 77 (2017) 367
Z	13	3.2	$\sigma = 58.43 \pm 0.03 \pm 1.66$ nb	$\sigma = 55.96 + 1.5 - 1.7$ nb (DYNNLO+CT14 NNLO)	JHEP 02 (2017) 117
Z	8	20.2	$\sigma = 34.24 \pm 0.03 \pm 0.92$ nb	$\sigma = 32.94 + 0.8 - 0.92$ nb (DYNNLO+CT14 NNLO)	JHEP 02 (2017) 117
Z	7	4.6	$\sigma = 29.53 \pm 0.03 \pm 0.77$ nb	$\sigma = 28.31 + 0.68 - 0.8$ nb (DYNNLO+CT14 NNLO)	JHEP 02 (2017) 117
$t\bar{t}$	13	36.1	$\sigma = 826.4 \pm 3.6 \pm 19.6$ pb	$\sigma = 832 + 40 - 45$ pb (top++ NNLO+NNLL)	EPJC 80 (2020) 528
$t\bar{t}$	8	20.2	$\sigma = 242.9 \pm 1.7 \pm 8.6$ pb	$\sigma = 252.9 + 13.3 - 14.5$ pb (top++ NNLO+NNLL)	EPJC 74 (2014) 3109
$t\bar{t}$	7	4.6	$\sigma = 182.9 \pm 3.1 \pm 6.4$ pb	$\sigma = 177 + 10 - 11$ pb (top++ NNLO+NNLL)	EPJC 74 (2014) 3109
t_{t-chan}	13	3.2	$\sigma = 247 \pm 6 \pm 46$ pb	$\sigma = 217 \pm 10$ pb (NLO+NLL)	JHEP 04 (2017) 086
t_{t-chan}	8	20.3	$\sigma = 89.6 \pm 1.7 + 7.2 - 6.4$ pb	$\sigma = 87.8 + 3.4 - 1.9$ pb (NLO+NLL)	EPJC 77 (2017) 531
t_{t-chan}	7	4.6	$\sigma = 68 \pm 2 \pm 8$ pb	$\sigma = 64.6 + 2.7 - 2$ pb (NLO+NLL)	PRD 90, 112006 (2014)
Wt	13	3.2	$\sigma = 94 \pm 10 + 28 - 23$ pb	$\sigma = 71.7 \pm 3.9$ pb (NLO+NNLL)	JHEP 01 (2018) 63
Wt	8	20.3	$\sigma = 23 \pm 1.3 + 3.4 - 3.7$ pb	$\sigma = 22.4 \pm 1.5$ pb (NLO+NLL)	JHEP 01, 064 (2016)
Wt	7	2.0	$\sigma = 16.8 \pm 2.9 \pm 3.9$ pb	$\sigma = 15.7 \pm 1.1$ pb (NLO+NLL)	PLB 716, 142-159 (2012)
H	13	139	$\sigma = 55.5 \pm 3.2 + 2.4 - 2.2$ pb	$\sigma = 55.6 \pm 2.5$ pb (LHC-HXSWG YR4)	ATLAS-CONF-2022-002
H	8	20.3	$\sigma = 27.7 \pm 3 + 2.3 - 1.9$ pb	$\sigma = 24.5 + 1.3 - 1.8$ pb (LHC-HXSWG YR4)	EPJC 76 (2016) 6
H	7	4.5	$\sigma = 22.1 + 6.7 - 5.3 + 3.3 - 2.7$ pb	$\sigma = 19.2 + 1 - 1.4$ pb (LHC-HXSWG YR4)	EPJC 76 (2016) 6
H VBF, $\lvert y_H\rvert < 2.5$	13	139	$\sigma = 4 \pm 0.3 + 0.3 - 0.4$ pb	$\sigma = 3.51 \pm 0.07$ pb (LHC-HXSWG)	ATLAS-CONF-2021-053
H VBF	8	20.3	$\sigma = 2.43 + 0.5 - 0.49 + 0.33 - 0.26$ pb	$\sigma = 1.6 \pm 0.04$ pb (LHC-HXSWG YR4)	EPJC 76 (2016) 6
VH	8	20.3	$\sigma = 1.03 + 0.37 - 0.36 + 0.26 - 0.21$ pb	$\sigma = 1.12 \pm 0.03$ pb (NNLO(QCD)+NLO(EW))	JHEP 12 (2017) 024
WH, $\lvert y_H\rvert < 2.5$	13	139	$\sigma = 1.56 + 0.2 - 0.21 + 0.16 - 0.18$ pb	$\sigma = 1.203 \pm 0.024$ pb (Powheg Box NLO(QCD))	ATLAS-CONF-2021-053
ZH, $\lvert y_H\rvert < 2.5$	13	139	$\sigma = 0.7 \pm 0.13 + 0.1 - 0.12$ pb	$\sigma = 0.795 \pm 0.03$ pb (Powheg Box NLO(QCD))	ATLAS-CONF-2021-053
$t\bar{t}H$	13	139	$\sigma = 560 \pm 80 + 70 - 80$ fb	$\sigma = 580 \pm 50$ fb (LHCHXSWG NLO QCD + NLO EW)	ATLAS-CONF-2021-053
$t\bar{t}H$	8	20.3	$\sigma = 220 \pm 100 \pm 70$ fb	$\sigma = 133 + 8 - 13$ fb (LHCHXSWG NLO QCD + NLO EW)	PLB 784 (2018) 173
WW	13	36.1	$\sigma = 130.04 \pm 1.7 \pm 10.6$ pb	$\sigma = 128.4 + 3.2 - 2.9$ pb (NNLO)	EPJC 79 (2019) 884
WW	8	20.3	$\sigma = 68.2 \pm 1.2 \pm 4.6$ pb	$\sigma = 65 + 1.2 - 1.1$ pb (NNLO)	PLB 763, 114 (2016)
WW	7	4.6	$\sigma = 51.9 \pm 2 \pm 4.4$ pb	$\sigma = 49.04 + 1.03 - 0.88$ pb (NNLO)	Phys. Rev. D 87 (2013) 112001, arXiv:1408.5243
WZ	13	36.1	$\sigma = 51 \pm 0.8 \pm 2.3$ pb	$\sigma = 49.1 + 1.1 - 1$ pb (MATRIX (NNLO))	EPJC 79 (2019) 535
WZ	8	20.3	$\sigma = 24.3 \pm 0.6 \pm 0.9$ pb	$\sigma = 23.92 \pm 0.4$ pb (MATRIX (NNLO))	PRD 93, 092004 (2016)
WZ	7	4.6	$\sigma = 19 + 1.4 - 1.3 \pm 1$ pb	$\sigma = 19.34 + 0.3 - 0.4$ pb (MATRIX (NNLO))	EPJC 72 (2012) 2173
ZZ	13	36.1	$\sigma = 17.3 \pm 0.6 \pm 0.8$ pb	$\sigma = 16.9 + 0.6 - 0.5$ pb (Matrix (NNLO) & Sherpa (NLO))	PRD 97 (2018) 032005
ZZ	8	20.3	$\sigma = 7.3 \pm 0.4 + 0.4 - 0.3$ pb	$\sigma = 8.284 + 0.249 - 0.191$ pb (NNLO)	JHEP 01, 099 (2017)
ZZ	7	4.6	$\sigma = 6.7 \pm 0.7 + 0.5 - 0.4$ pb	$\sigma = 6.735 + 0.195 - 0.155$ pb (NNLO)	JHEP 03, 128 (2013), PLB 735 (2014) 311
t_{s-chan}	8	20.3	$\sigma = 4.8 \pm 0.8 + 1.6 - 1.3$ pb	$\sigma = 5.61 \pm 0.22$ pb (NLO+NNL)	LB 756, 228-246 (2016)
$t\bar{t}W$	13	36.1	$\sigma = 870 \pm 130 \pm 140$ fb	$\sigma = 600 \pm 72$ fb (Madgraph5 + aMCNLO)	PRD 99, 072009 (2019)
$t\bar{t}W$	8	20.3	$\sigma = 369 + 86 - 79 \pm 44$ fb	$\sigma = 232 \pm 32$ fb (MCFM)	JHEP 11, 172 (2015)
$t\bar{t}Z$	13	139	$\sigma = 990 \pm 50 \pm 80$ fb	$\sigma = 840 \pm 90$ fb (Madgraph5 + aMCNLO)	Eur. Phys. J. C 81 (2021) 737
$t\bar{t}Z$	8	20.3	$\sigma = 176 + 52 - 48 \pm 24$ fb	$\sigma = 215 \pm 30$ fb (HELAC-NLO)	JHEP 11, 172 (2015)
WWW	13	139	$\sigma = 0.82 \pm 0.01 \pm 0.08$ pb	$\sigma = 0.511 \pm 0.018$ pb (NLO QCD)	arXiv:2201.13045
WWZ	13	79.8	$\sigma = 0.55 \pm 0.14 + 0.15 - 0.13$ pb	$\sigma = 0.358 \pm 0.036$ pb (Sherpa 2.2.2)	PLB 798 (2019) 134913
$t\bar{t}t\bar{t}$	13	139	$\sigma = 24 \pm 4 \pm 5$ fb	$\sigma = 12 \pm 2.4$ fb (NLO QCD + EW)	JHEP 11 (2021) 118

(b)

Figure 1: Summary of several Standard Model cross-section measurements (a) with associated references (b). The measurements are corrected for branching fractions, compared to the corresponding theoretical expectations.

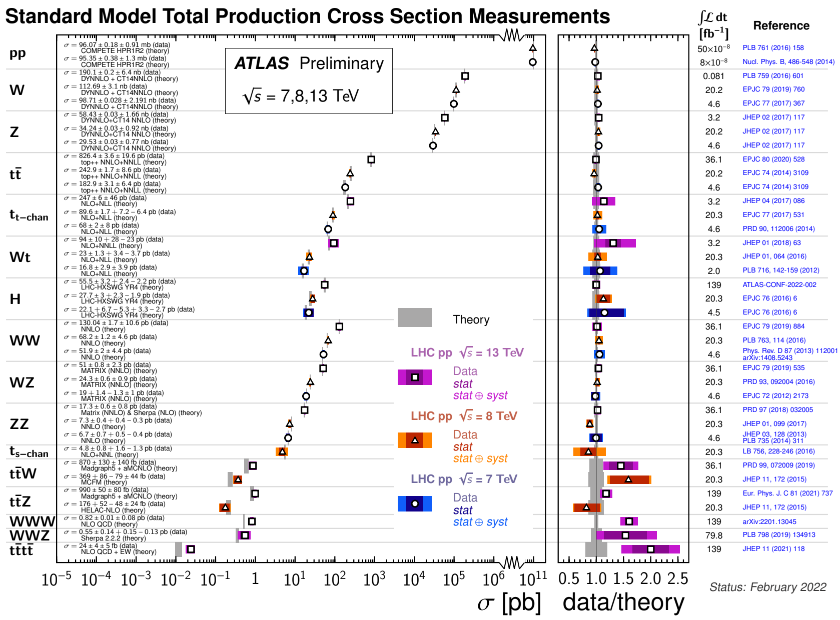

Figure 2: Summary of several Standard Model total production cross-section measurements, corrected for branching fractions, compared to the corresponding theoretical expectations and ratio with respect to theory. The associated references can also be found in Table 1(b).

4 Fiducial cross section overview plots

Figures 3, 4, 5, 6, 7, 8, 9, 10 and 11 summarize several Standard Model total and fiducial production cross-section measurements, corrected for branching fractions, compared to the corresponding theoretical expectations. For the measurement of the tZj production process at 13 TeV, the fiducial volume definition was updated to require $m_{\ell\ell} > 30$ GeV. Some measurements have been extrapolated using branching ratios as predicted by the Standard Model for the Higgs boson. Uncertainties for the theoretical predictions are quoted from the original ATLAS papers. They were not always evaluated using the same prescriptions for PDFs and scales.

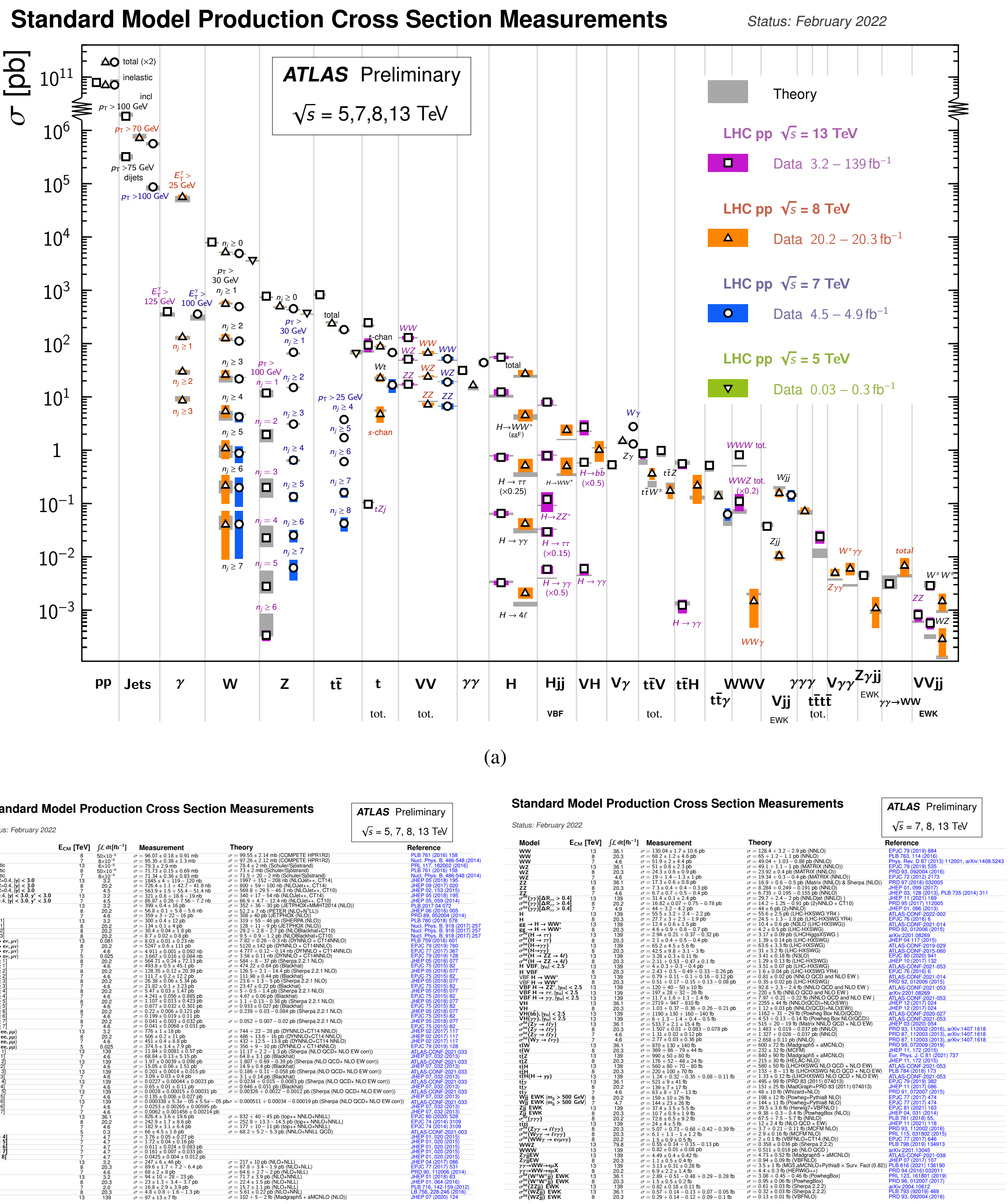

Figure 3: Summary of several Standard Model total and fiducial production cross-section measurements (a) with associated references (b) and (c). The measurements are corrected for branching fractions, compared to the corresponding theoretical expectations. In some cases, the fiducial selection is different between measurements in the same final state for different centre-of-mass energies $\sqrt{s}$, resulting in lower cross section values at higher $\sqrt{s}$.

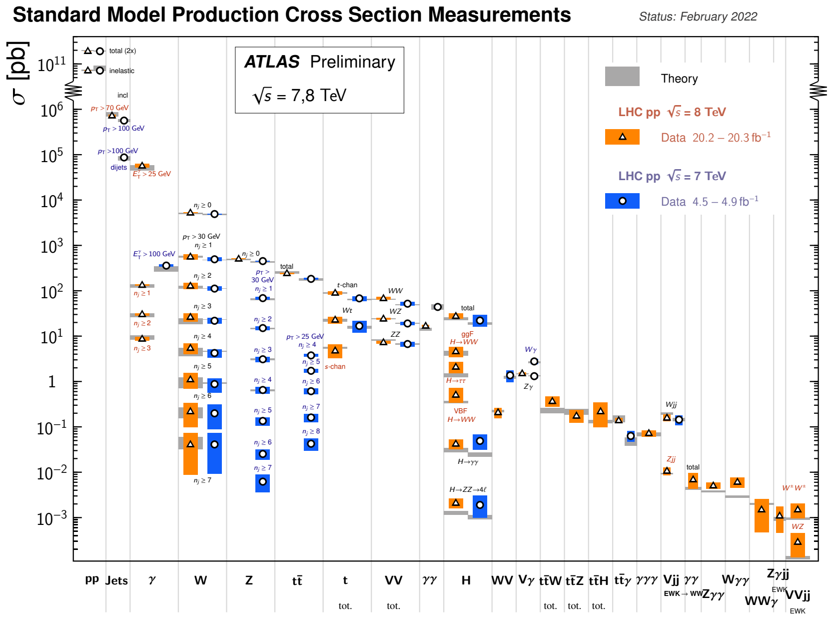

Figure 4: Summary of several Standard Model total and fiducial production cross-section measurements from Run 1, corrected for branching fractions, compared to the corresponding theoretical expectations. In some cases, the fiducial selection is different between measurements in the same final state for different centre-of-mass energies $\sqrt{s}$, resulting in lower cross section values at higher $\sqrt{s}$. The associated references can be found in Table 3(b) and 3(c).

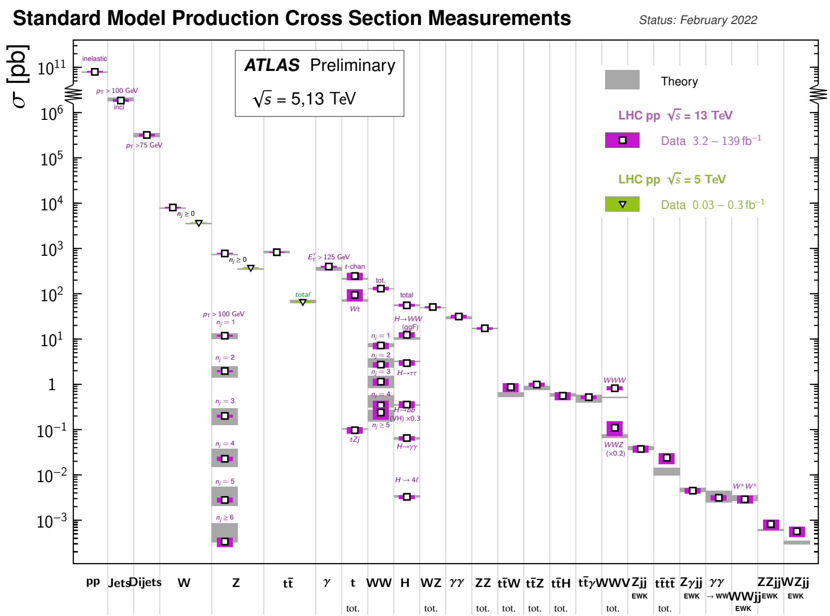

Figure 5: Summary of several Standard Model total and fiducial production cross-section measurements from Run 2, corrected for branching fractions, compared to the corresponding theoretical expectations. The associated references can be found in Table 3(b) and 3(c).

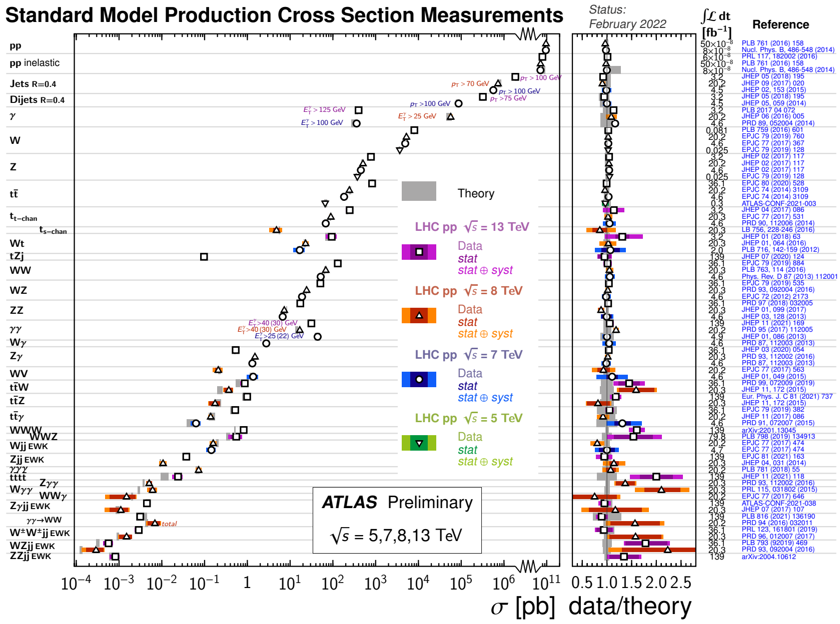

Figure 6: Summary of several Standard Model total and fiducial production cross-section measurements, corrected for branching fractions, compared to the corresponding theoretical expectations and ratio with respect to theory. In some cases, the fiducial selection is different between measurements in the same final state for different centre-of-mass energies $\sqrt{s}$, resulting in lower cross section values at higher $\sqrt{s}$.

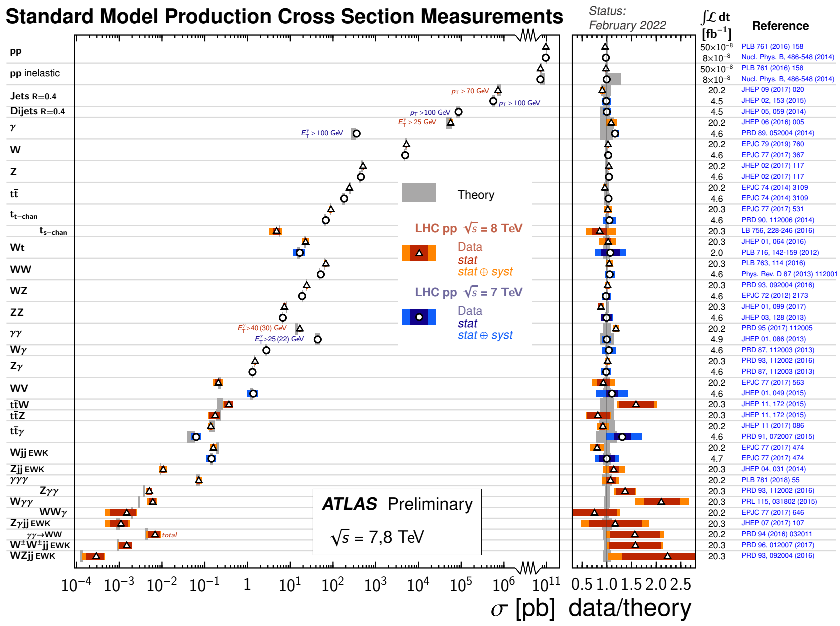

Figure 7: Summary of several Standard Model total and fiducial production cross-section measurements from Run 1, corrected for branching fractions, compared to the corresponding theoretical expectations and ratio with respect to theory. In some cases, the fiducial selection is different between measurements in the same final state for different centre-of-mass energies $\sqrt{s}$, resulting in lower cross section values at higher $\sqrt{s}$.

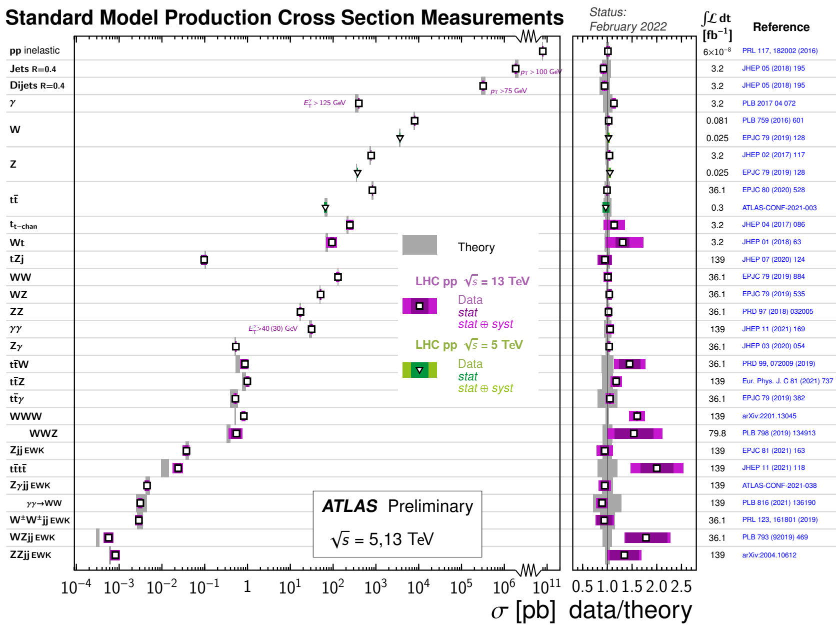

Figure 8: Summary of several Standard Model total and fiducial production cross-section measurements from Run 2, corrected for branching fractions, compared to the corresponding theoretical expectations and ratio with respect to theory.

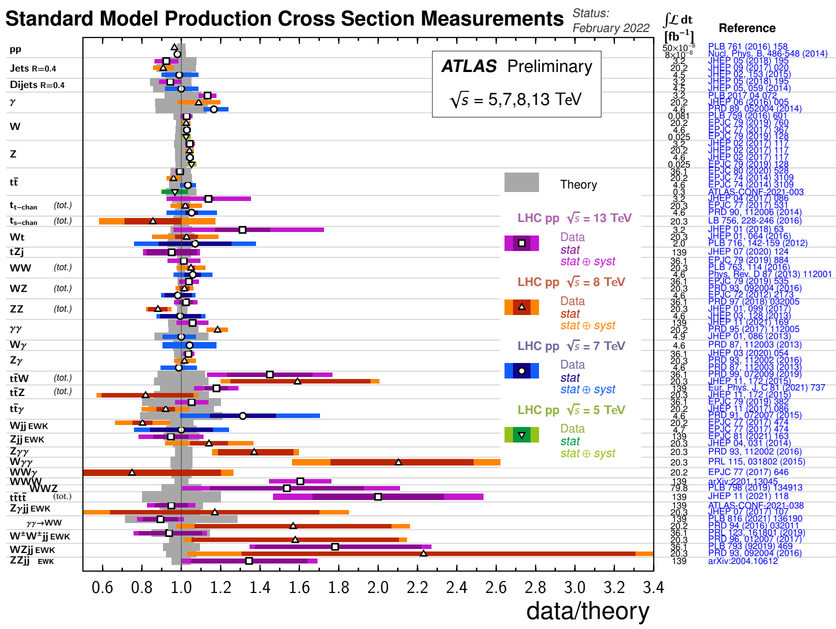

Figure 9: Summary of ratios with respect to theory for several Standard Model total and fiducial production cross-section measurements, corrected for branching fractions.

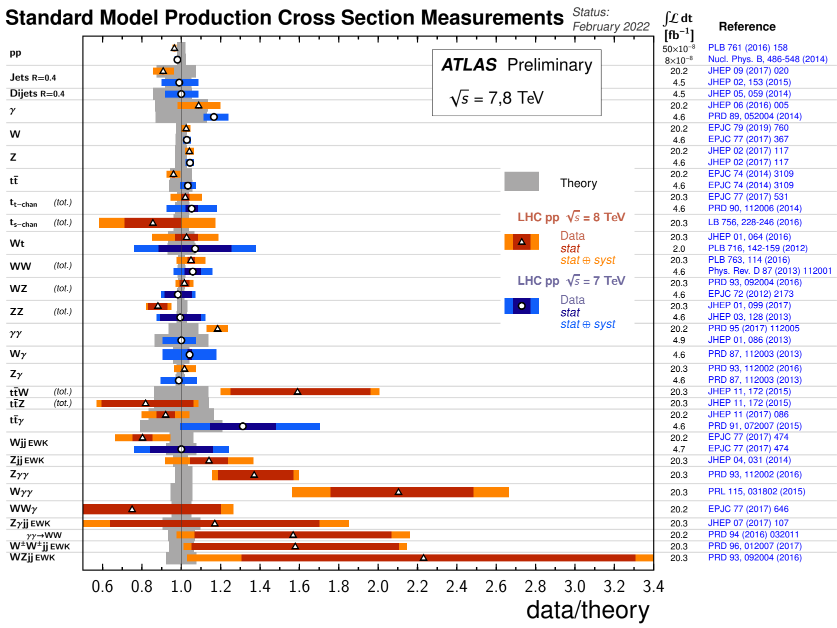

Figure 10: Summary of ratios with respect to theory for several Standard Model total and fiducial production cross-section measurements from Run 1, corrected for branching fractions.

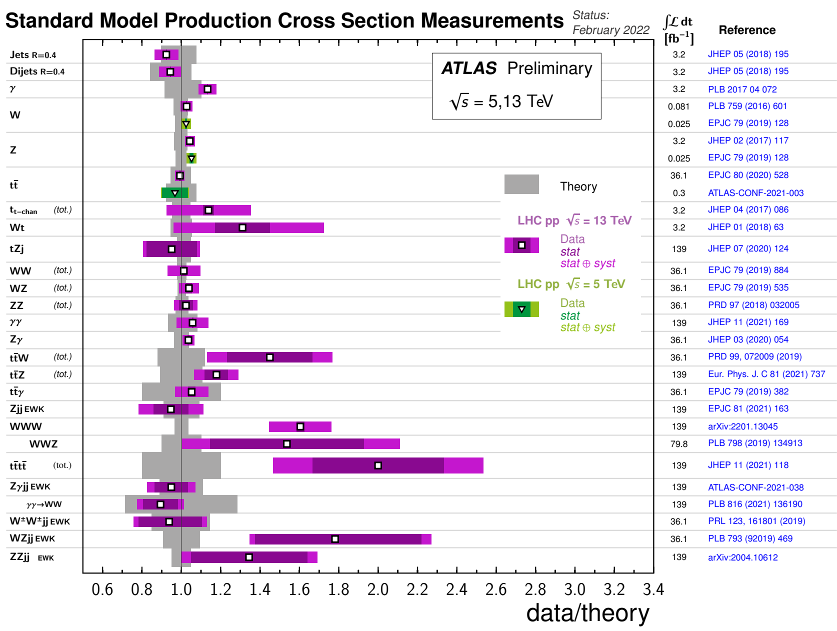

Figure 11: Summary of ratios with respect to theory for several Standard Model total and fiducial production cross-section measurements from Run 2, corrected for branching fractions.

5 Overview plots for inclusive measurements

Figures 12, 13, 14 show the data/theory ratio for several inclusive jet fiducial production cross-section measurements. All theoretical expectations were calculated at NLO or higher. The dark-color error bar represents the statistical uncertainty. The lighter-color error bar represents the full uncertainty, including systematics and luminosity uncertainties. The luminosity used and reference for each measurement are also shown. Uncertainties for the theoretical predictions are quoted from the original ATLAS papers.

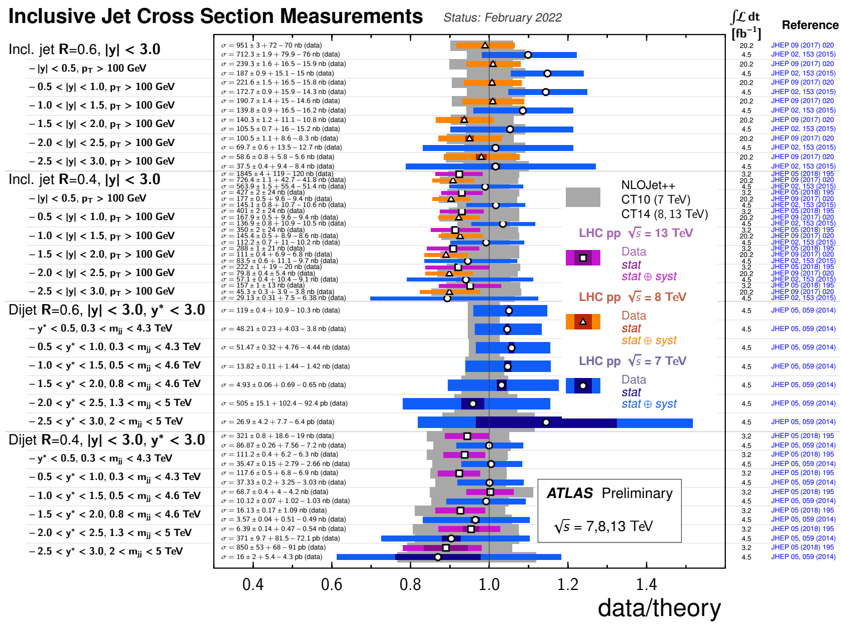

Figure 12: The data/theory ratio for several inclusive jet fiducial production cross-section measurements.

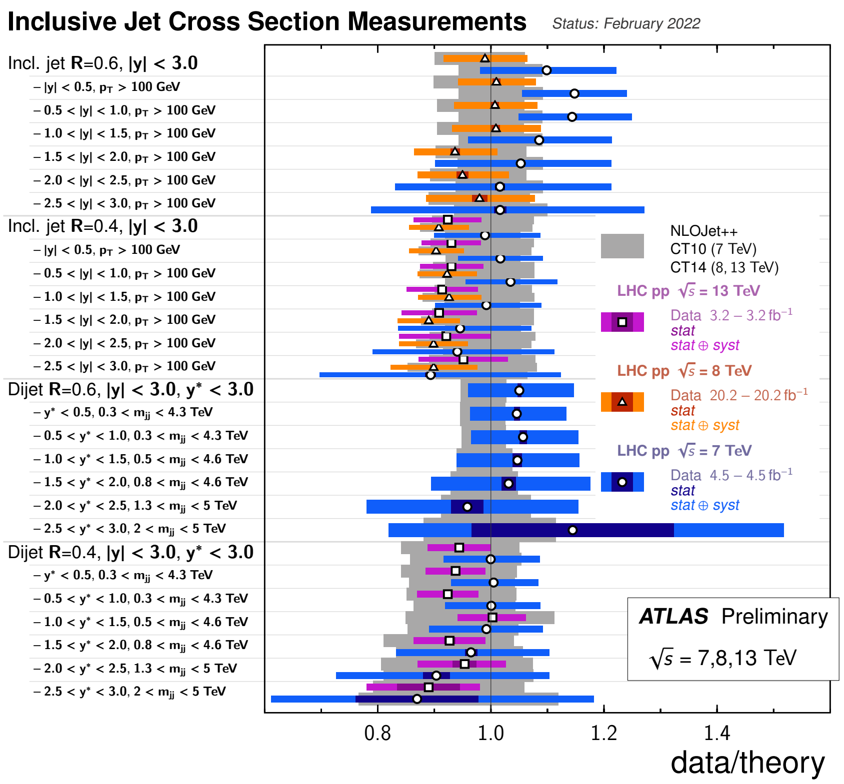

Figure 13: The data/theory ratio for several inclusive jet fiducial production cross-section measurements.

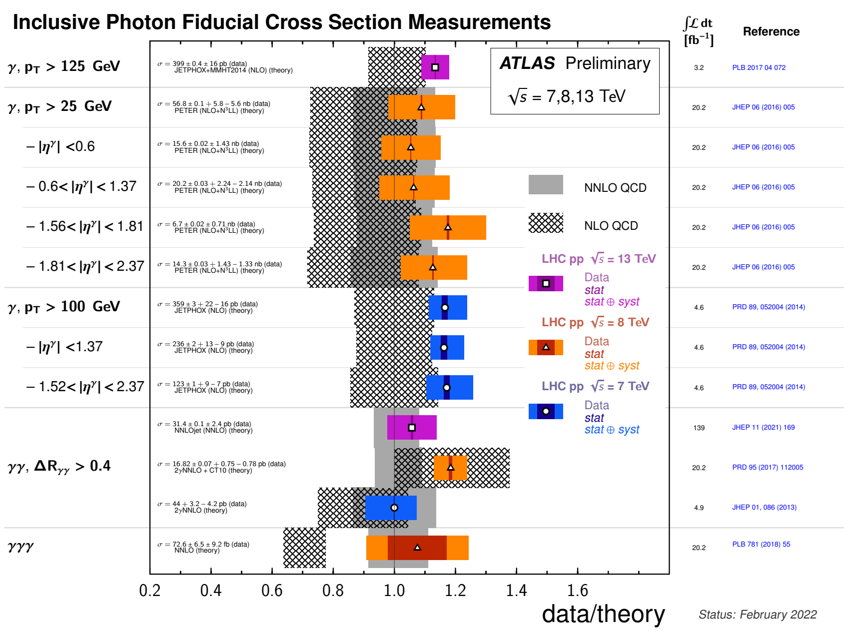

Figure 14: The ratio for several inclusive photon fiducial production cross-section measurements over theory prediction. All theoretical expectations are shown using gray bars, hatched for NLO calculations and full for NNLO predictions.

6 Overview plots for single boson measurements

Figures 15 and 16 show the data/theory ratio for several single-boson fiducial production cross-section measurements, corrected for branching fractions. All theoretical expectations were calculated at NLO or higher. The dark-color error bar represents the statistical uncertainly. The lighter-color error bar represents the full uncertainty, including systematics and luminosity uncertainties. The luminosity used and reference for each measurement are also shown. Uncertainties for the theoretical predictions are quoted from the original ATLAS papers. They were not always evaluated using the same prescriptions for PDFs and scales.

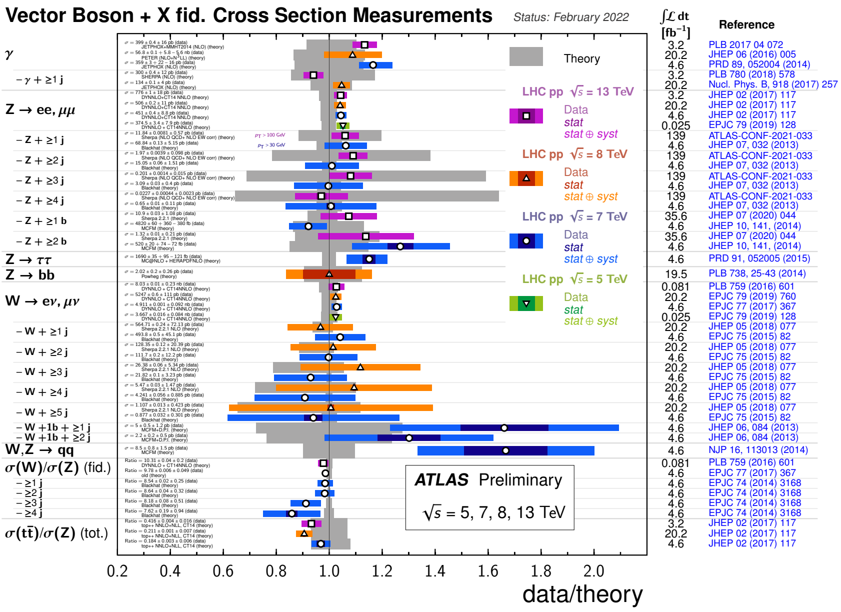

Figure 15: The data/theory ratio for several single-boson fiducial production cross-section measurements, corrected for branching fractions.

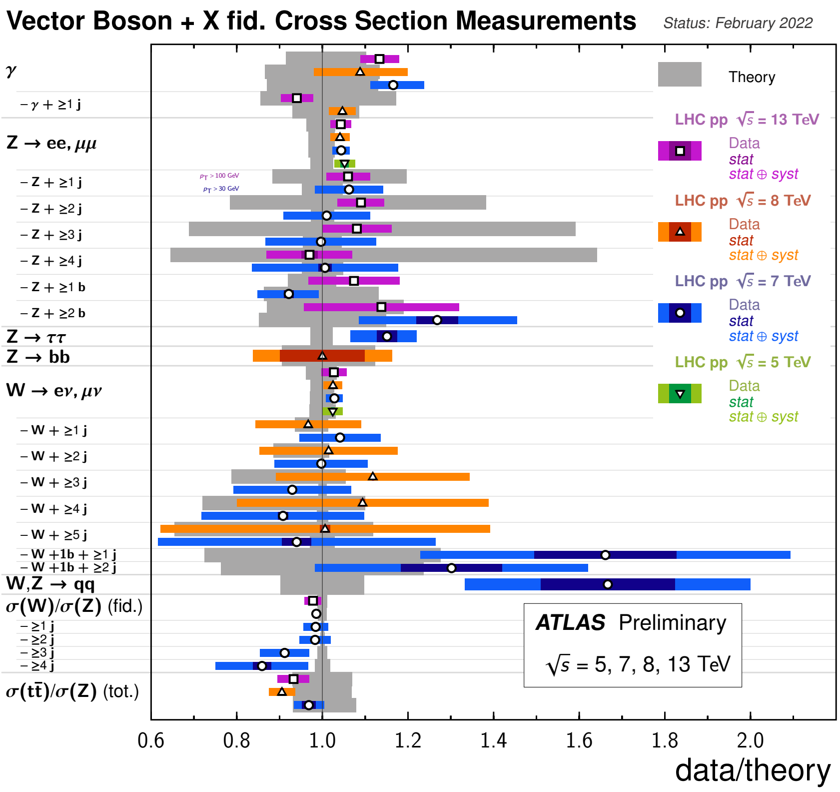

Figure 16: The data/theory ratio for several single-boson fiducial production cross-section measurements, corrected for branching fractions.

7 Overview plots for diboson measurements

Figures 17 and 18 show the ratio for several diboson total and fiducial production cross-section measurements over theory prediction, corrected for branching fractions. All theoretical expectations are shown using gray bars, hatched for NLO calculations and full for NNLO predictions. The dark-color error bar represents the statistical uncertainly. The lighter-color error bar represents the full uncertainty, including systematics and luminosity uncertainties. The luminosity used and reference for each measurement are also shown. Uncertainties for the theoretical predictions are quoted from the original ATLAS papers.

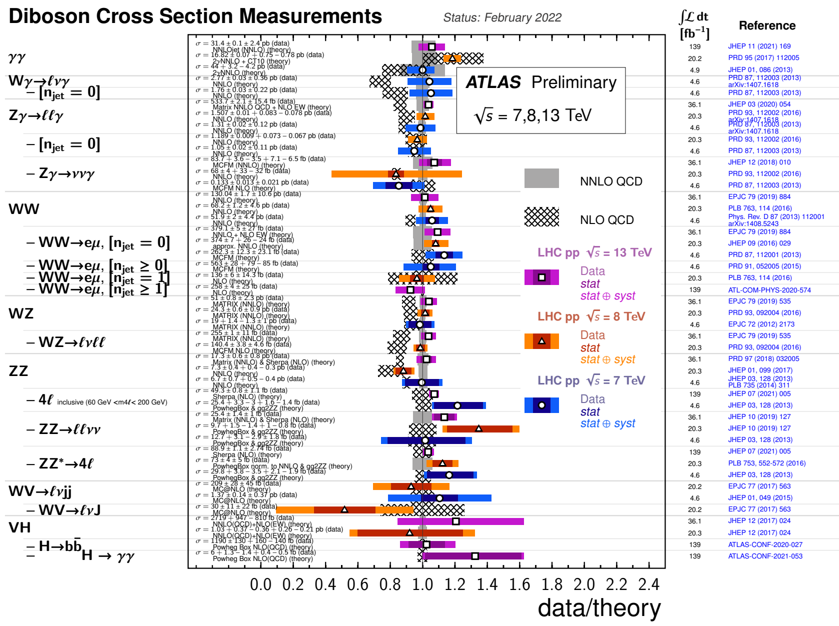

Figure 17: The data/theory ratio for several diboson fiducial production cross-section measurements, corrected for branching fractions.

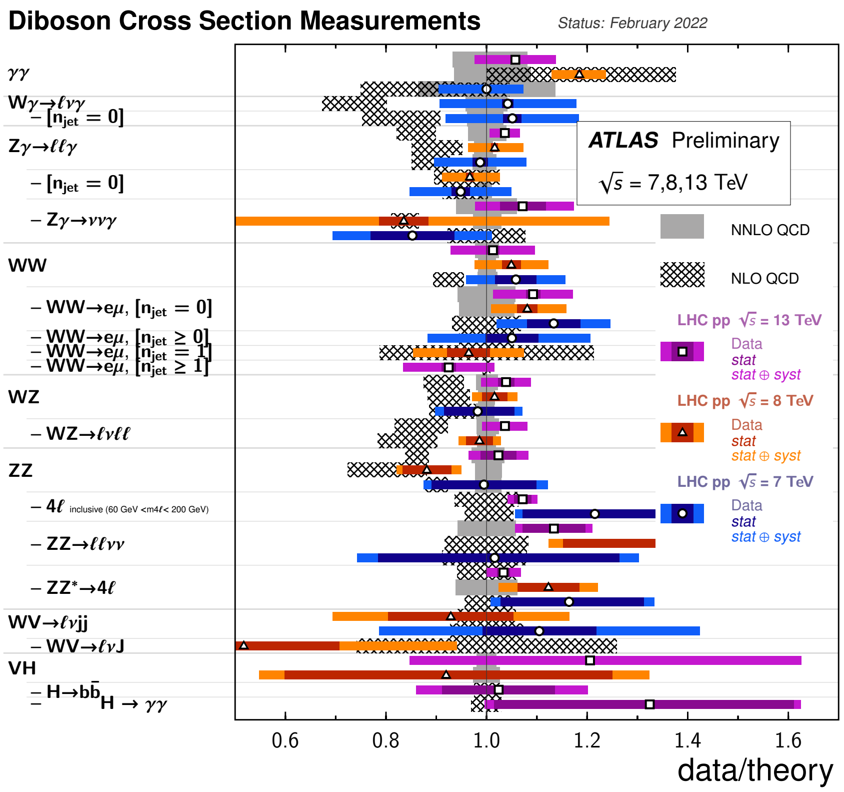

Figure 18: The data/theory ratio for several diboson fiducial production cross-section measurements, corrected for branching fractions.

8 Overview plots for VBF, VBS and triboson measurements

Figures 19 and 20 show the data/theory ratio for several vector boson fusion, vector boson scattering, and triboson fiducial cross-section measurements. The dark-color error bar represents the statistical uncertainty. The lighter-color error bar represents the full uncertainty, including systematics and luminosity uncertainties. The luminosity used and reference for each measurement are also shown. Uncertainties for the theoretical predictions are quoted from the original ATLAS papers. They were not always evaluated using the same prescriptions for PDFs and scales.

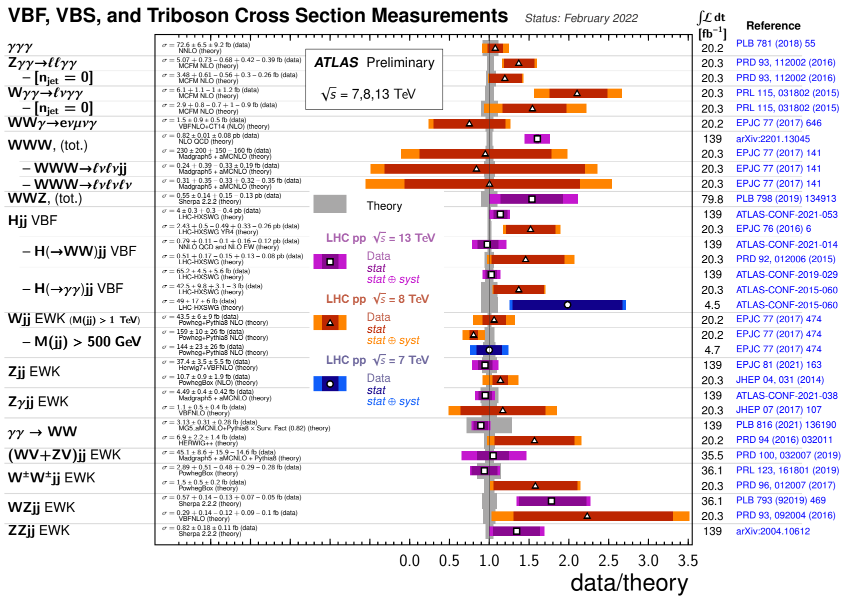

Figure 19: The data/theory ratio for several vector boson fusion, vector boson scattering, and triboson fiducial production cross-section measurements.

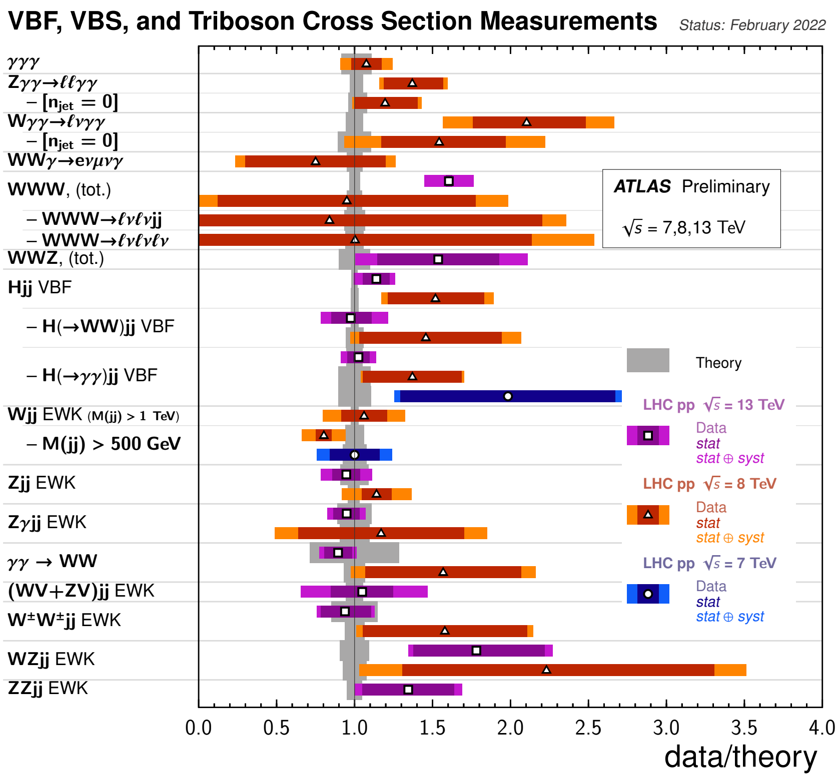

Figure 20: The data/theory ratio for several vector boson fusion, vector boson scattering, and triboson fiducial production cross-section measurements.

9 Used values

Figures 21, 22, 23, and 24 present tables of used results. Uncertainties for the theoretical predictions are quoted from the original ATLAS papers. They were not always evaluated using the same prescriptions for PDFs and scales.

Standard Model Production Cross Section Measurements I

Status: February 2022

ATLAS Preliminary

$\sqrt{s}$ = 7, 8, 13 TeV

Model	E_{CM} [TeV]	$\int\mathcal{L}\,dt[fb^{-1}]$	Measurement	Theory	Reference
H	13	139	$\sigma = 55.5 \pm 3.2 + 2.4 - 2.2$ pb	$\sigma = 55.6 \pm 2.5$ pb (LHC-HXSWG YR4)	ATLAS-CONF-2022-002
H	8	20.3	$\sigma = 27.7 \pm 3 + 2.3 - 1.9$ pb	$\sigma = 24.5 + 1.3 - 1.8$ pb (LHC-HXSWG YR4)	EPJC 76 (2016) 6
H	7	4.5	$\sigma = 22.1 + 6.7 - 5.3 + 3.3 - 2.7$ pb	$\sigma = 19.2 + 1 - 1.4$ pb (LHC-HXSWG YR4)	EPJC 76 (2016) 6
H ggF, $\lvert y_H\rvert < 2.5$	13	139	$\sigma = 45.7 + 1.7 - 1.8 + 2.2 - 2.7$ pb	$\sigma = 44.8 \pm 2.6$ pb (LHC-HXSWG)	ATLAS-CONF-2021-053
H ggF	8	20.3	$\sigma = 23.9 \pm 3.1 + 2.1 - 1.9$ pb	$\sigma = 21.4 + 1.2 - 1.6$ pb (LHC-HXSWG YR4)	EPJC 76, 6 (2016)
H VBF, $\lvert y_H\rvert < 2.5$	13	139	$\sigma = 4 \pm 0.3 + 0.3 - 0.4$ pb	$\sigma = 3.51 \pm 0.07$ pb (LHC-HXSWG)	ATLAS-CONF-2021-053
H VBF	8	20.3	$\sigma = 2.43 + 0.5 - 0.49 + 0.33 - 0.26$ pb	$\sigma = 1.6 \pm 0.04$ pb (LHC-HXSWG YR4)	EPJC 76 (2016) 6
WH, $\lvert y_H\rvert < 2.5$	13	139	$\sigma = 1.56 + 0.2 - 0.21 + 0.16 - 0.18$ pb	$\sigma = 1.203 \pm 0.024$ pb (Powheg Box NLO(QCD))	ATLAS-CONF-2021-053
ZH, $\lvert y_H\rvert < 2.5$	13	139	$\sigma = 0.7 \pm 0.13 + 0.1 - 0.12$ pb	$\sigma = 0.795 \pm 0.03$ pb (Powheg Box NLO(QCD))	ATLAS-CONF-2021-053
VH	13	36.1	$\sigma = 2719 + 947 - 810$ fb	$\sigma = 2255 \pm 44$ fb (NNLO(QCD)+NLO(EW))	JHEP 12 (2017) 024
VH	8	20.3	$\sigma = 1.03 + 0.37 - 0.36 + 0.26 - 0.21$ pb	$\sigma = 1.12 \pm 0.03$ pb (NNLO(QCD)+NLO(EW))	JHEP 12 (2017) 024
VH($b\bar{b}$), $\lvert y_H\rvert < 2.5$	13	139	$\sigma = 1190 \pm 130 + 160 - 140$ fb	$\sigma = 1162 + 31 - 29$ fb (Powheg Box NLO(QCD))	ATLAS-CONF-2020-027
VH($\gamma\gamma$), $\lvert y_H\rvert < 2.5$	13	139	$\sigma = 6 + 1.3 - 1.4 + 0.4 - 0.5$ fb	$\sigma = 4.53 + 0.13 - 0.14$ fb (Powheg Box NLO(QCD))	ATLAS-CONF-2021-053
$t\bar{t}H$	13	139	$\sigma = 560 \pm 80 + 70 - 80$ fb	$\sigma = 580 \pm 50$ fb (LHCHXSWG NLO QCD + NLO EW)	ATLAS-CONF-2021-053
$t\bar{t}H$	8	20.3	$\sigma = 220 \pm 100 \pm 70$ fb	$\sigma = 133 + 8 - 13$ fb (LHCHXSWG NLO QCD + NLO EW)	PLB 784 (2018) 173
$\sigma^{fid}(H\to\gamma\gamma)$	13	139	$\sigma = 65.2 \pm 4.5 \pm 5.6$ fb	$\sigma = 63.6 \pm 3.3$ fb (LHC-HXSWG)	ATLAS-CONF-2019-029
$\sigma^{fid}(H\to\gamma\gamma)$	8	20.3	$\sigma = 42.5 \pm 9.8 + 3.1 - 3$ fb	$\sigma = 31 \pm 3.2$ fb (LHC-HXSWG)	ATLAS-CONF-2015-060
$\sigma^{fid}(H\to\gamma\gamma)$	7	4.5	$\sigma = 49 \pm 17 \pm 6$ fb	$\sigma = 24.7 \pm 2.6$ fb (LHC-HXSWG)	ATLAS-CONF-2015-060
VBF $H \to WW^*$	13	139	$\sigma = 0.79 + 0.11 - 0.1 + 0.16 - 0.12$ pb	$\sigma = 0.81 \pm 0.02$ pb (NNLO QCD and NLO EW)	ATLAS-CONF-2021-014
VBF $H \to WW^*$	8	20.3	$\sigma = 0.51 + 0.17 - 0.15 + 0.13 - 0.08$ pb	$\sigma = 0.35 \pm 0.02$ pb (LHC-HXSWG)	PRD 92, 012006 (2015)
VBF $H \to ZZ^*$, $\lvert y_H\rvert < 2.5$	13	139	$\sigma = 120 + 40 - 50 \pm 10$ fb	$\sigma = 92.8 + 2.3 - 2.4$ fb (NNLO QCD and NLO EW)	ATLAS-CONF-2021-053
VBF $H \to \tau\tau$, $\lvert y_H\rvert < 2.5$	13	139	$\sigma = 197 \pm 28 + 32 - 26$ fb	$\sigma = 220 \pm 5$ fb (NNLO QCD and NLO EW)	arXiv:2201.08269
VBF $H \to \gamma\gamma$, $\lvert y_H\rvert < 2.5$	13	139	$\sigma = 11.7 \pm 1.6 + 1.1 - 1.4$ fb	$\sigma = 7.97 + 0.21 - 0.22$ fb (NNLO QCD and NLO EW)	ATLAS-CONF-2021-053
$gg \to H \to WW^*$	13	139	$\sigma = 12.4 \pm 0.6 \pm 1.5$ pb	$\sigma = 10.4 \pm 0.6$ pb (N3LO (LHC-HXSWG))	ATLAS-CONF-2021-014
$gg \to H \to WW^*$	8	20.3	$\sigma = 4.6 \pm 0.9 + 0.8 - 0.7$ pb	$\sigma = 4.2 \pm 0.5$ pb (LHC-HXSWG)	PRD 92, 012006 (2015)
$gg \to H \to WW^*$	7	4.5	$\sigma = 2 \pm 1.7 + 1.2 - 1.1$ pb	$\sigma = 3.3 \pm 0.4$ pb (LHC-HXSWG)	PRD 92, 012006 (2015)
$\sigma^{fid}(H \to ZZ \to 4\ell)$	13	139	$\sigma = 3.28 \pm 0.3 \pm 0.11$ fb	$\sigma = 3.41 \pm 0.18$ fb (N3LO)	EPJC 80 (2020) 941
$\sigma^{fid}(H \to ZZ \to 4\ell)$	8	20.3	$\sigma = 2.11 + 0.53 - 0.47 \pm 0.1$ fb	$\sigma = 1.29 \pm 0.13$ fb (LHC-HXSWG)	JHEP 10 (2017) 132
$\sigma^{fid}(H \to ZZ \to 4\ell)$	7	4.5	$\sigma = 1.9 + 1.2 - 0.9 \pm 0.1$ fb	$\sigma = 1.03 \pm 0.11$ fb (LHC-HXSWG)	JHEP 10 (2017) 132
$\sigma^{fid}(H \to \tau\tau)$	13	139	$\sigma = 2.94 \pm 0.21 + 0.37 - 0.32$ pb	$\sigma = 3.17 \pm 0.09$ pb (LHCHiggsXSWG)	arXiv:2201.08269
$\sigma^{fid}(H \to \tau\tau)$	8	20.3	$\sigma = 2.1 \pm 0.4 + 0.5 - 0.4$ pb	$\sigma = 1.39 \pm 0.14$ pb (LHC-HXSWG)	JHEP 04 117 (2015)
$\sigma^{fid}(H \to \tau\tau)$	7	4.5	$\sigma = 1 + 0.9 - 0.8 + 0.9 - 0.8$ pb	$\sigma = 1.09 \pm 0.11$ pb (LHC-HXSWG)	JHEP 04 117 (2015)
WW	13	36.1	$\sigma = 130.04 \pm 1.7 \pm 10.6$ pb	$\sigma = 128.4 + 3.2 - 2.9$ pb (NNLO)	EPJC 79 (2019) 884
WW	8	20.3	$\sigma = 68.2 \pm 1.2 \pm 4.6$ pb	$\sigma = 65 + 1.2 - 1.1$ pb (NNLO)	PLB 763, 114 (2016)
WW	7	4.6	$\sigma = 51.9 \pm 2 \pm 4.4$ pb	$\sigma = 49.04 + 1.03 - 0.88$ pb (NNLO)	Phys. Rev. D 87 (2013) 112001, arXiv:1408.5243
$\sigma^{fid}(WW\to e\mu)$ $[n_{jet}\geq0]$	7	4.6	$\sigma = 563 \pm 28 + 79 - 85$ fb	$\sigma = 536 \pm 29$ fb (MCFM)	PRD 91, 052005 (2015)
$\sigma^{fid}(WW\to e\mu)$ $[n_{jet}=1]$	8	20.3	$\sigma = 136 \pm 6 \pm 14.3$ fb	$\sigma = 141 \pm 30$ fb (NLO)	PLB 763, 114 (2016)
$\sigma^{fid}(WW\to e\mu)$ $[n_{jet}\geq1]$	13	139	$\sigma = 258 \pm 4 \pm 25$ fb	$\sigma = 279 \pm 2$ fb (NLO)	ATL-COM-PHYS-2020-574
$\sigma^{fid}(WW\to e\mu)$ $[n_{jet}=0]$	13	36.1	$\sigma = 379.1 \pm 5 \pm 27$ fb	$\sigma = 347 \pm 20$ fb (NNLO + NLO EW)	EPJC 79 (2019) 884
$\sigma^{fid}(WW\to e\mu)$ $[n_{jet}=0]$	8	20.3	$\sigma = 374 \pm 7 + 26 - 24$ fb	$\sigma = 346 \pm 19$ fb (approx. NNLO)	JHEP 09 (2016) 029
$\sigma^{fid}(WW\to e\mu)$ $[n_{jet}=0]$	7	4.6	$\sigma = 262.3 \pm 12.3 \pm 23.1$ fb	$\sigma = 231.4 \pm 15.7$ fb (MCFM)	PRD 87, 112001 (2013)
$\sigma^{fid}(WW\to\mu\mu)$ $[n_{jet}=0]$	8	20.3	$\sigma = 80.2 + 3.3 - 3.2 + 6.6 - 5.7$ fb	$\sigma = 71.2 \pm 4$ fb (NNLO)	JHEP 09 (2016) 029
$\sigma^{fid}(WW\to\mu\mu)$ $[n_{jet}=0]$	7	4.6	$\sigma = 73.9 \pm 5.9 \pm 7.5$ fb	$\sigma = 58.9 \pm 4$ fb (MCFM)	PRD 87, 112001 (2013)
$\sigma^{fid}(WW\to ee)$ $[n_{jet}=0]$	8	20.3	$\sigma = 73.4 + 4.2 - 4.1 + 6.7 - 5.8$ fb	$\sigma = 65.5 \pm 3.6$ fb (NNLO)	JHEP 09 (2016) 029
$\sigma^{fid}(WW\to ee)$ $[n_{jet}=0]$	7	4.6	$\sigma = 56.4 \pm 6.8 \pm 10$ fb	$\sigma = 54.6 \pm 3.7$ fb (MCFM)	PRD 87, 112001 (2013)
$\gamma\gamma\to WW\to e\mu X$	13	139	$\sigma = 3.13 \pm 0.31 \pm 0.28$ fb	$\sigma = 3.5 \pm 1$ fb (MG5_aMCNLO+Pythia8 $\times$ Surv. Fact (0.82))	PLB 816 (2021) 136190
$\gamma\gamma\to WW\to e\mu X$	8	20.2	$\sigma = 6.9 \pm 2.2 \pm 1.4$ fb	$\sigma = 4.4 \pm 0.3$ fb (HERWIG++)	PRD 94 (2016) 032011
$\sigma^{fid}(W^\pm W^\pm jj)$ EWK	13	36.1	$\sigma = 2.89 + 0.51 - 0.48 + 0.29 - 0.28$ fb	$\sigma = 3.08 + 0.45 - 0.46$ fb (PowhegBox)	PRL 123, 161801 (2019)
$\sigma^{fid}(W^\pm W^\pm jj)$ EWK	8	20.3	$\sigma = 1.5 \pm 0.5 \pm 0.2$ fb	$\sigma = 0.95 \pm 0.06$ fb (PowhegBox)	PRD 96, 012007 (2017)
WZ	13	36.1	$\sigma = 51 \pm 0.8 \pm 2.3$ pb	$\sigma = 49.1 + 1.1 - 1$ pb (MATRIX (NNLO))	EPJC 79 (2019) 535
WZ	8	20.3	$\sigma = 24.3 \pm 0.6 \pm 0.9$ pb	$\sigma = 23.92 \pm 0.4$ pb (MATRIX (NNLO))	PRD 93, 092004 (2016)
WZ	7	4.6	$\sigma = 19 + 1.4 - 1.3 \pm 1$ pb	$\sigma = 19.34 + 0.3 - 0.4$ pb (MATRIX (NNLO))	EPJC 72 (2012) 2173
$\sigma^{fid}(WZ \to \ell\nu\ell\ell)$	13	36.1	$\sigma = 255 \pm 1 \pm 11$ fb	$\sigma = 246 + 6 - 5$ fb (MATRIX (NNLO))	EPJC 79 (2019) 535
$\sigma^{fid}(WZ \to \ell\nu\ell\ell)$	8	20.3	$\sigma = 140.4 \pm 3.8 \pm 4.6$ fb	$\sigma = 142.4 + 2.6 - 2.7$ fb (MCFM NLO)	PRD 93, 092004 (2016)
$\sigma^{fid}(WZjj)$ EWK	13	36.1	$\sigma = 0.57 + 0.14 - 0.13 + 0.07 - 0.05$ fb	$\sigma = 0.32 \pm 0.03$ fb (Sherpa 2.2.2)	PLB 793 (92019) 469
$\sigma^{fid}(WZjj)$ EWK	8	20.3	$\sigma = 0.29 + 0.14 - 0.12 + 0.09 - 0.1$ fb	$\sigma = 0.13 \pm 0.01$ fb (VBFNLO)	PRD 93, 092004 (2016)
$WW+WZ\to\ell\nu J$	8	20.2	$\sigma = 30 \pm 11 \pm 22$ fb	$\sigma = 58 \pm 15$ fb (MC@NLO)	EPJC 77 (2017) 563
ZZ	13	36.1	$\sigma = 17.3 \pm 0.6 \pm 0.8$ pb	$\sigma = 16.9 + 0.6 - 0.5$ pb (Matrix (NNLO) & Sherpa (NLO))	PRD 97 (2018) 032005
ZZ	8	20.3	$\sigma = 7.3 \pm 0.4 + 0.4 - 0.3$ pb	$\sigma = 8.284 + 0.249 - 0.191$ pb (NNLO)	JHEP 01, 099 (2017)
ZZ	7	4.6	$\sigma = 6.7 \pm 0.7 + 0.5 - 0.4$ pb	$\sigma = 6.735 + 0.195 - 0.155$ pb (NNLO)	JHEP 03, 128 (2013), PLB 735 (2014) 311
$ZZ \to 4\ell$	8	20.3	$\sigma = 107 \pm 9 \pm 5$ fb	$\sigma = 104.9 \pm 1.7$ fb (Powheg)	PRL 112, 231806 (2014)
$ZZ \to 4\ell$	7	4.5	$\sigma = 76 \pm 18 \pm 4$ fb	$\sigma = 90 \pm 1.6$ fb (Powheg)	PRL 112, 231806 (2014)
$\sigma^{fid}(ZZ \to 4\ell)$	13	139	$\sigma = 49.3 \pm 0.8 \pm 1.1$ fb	$\sigma = 46 \pm 2.9$ fb (Sherpa (NLO))	JHEP 07 (2021) 005
$\sigma^{fid}(ZZ \to 4\ell)$	7	4.6	$\sigma = 25.4 + 3.3 - 3 + 1.6 - 1.4$ fb	$\sigma = 20.9 + 1.1 - 0.9$ fb (PowhegBox & gg2ZZ)	JHEP 03, 128 (2013)
$\sigma^{fid}(ZZ^* \to 4\ell)$	13	139	$\sigma = 88.9 \pm 1.1 \pm 2.74$ fb	$\sigma = 86 \pm 5$ fb (Sherpa (NLO))	JHEP 07 (2021) 005
$\sigma^{fid}(ZZ^* \to 4\ell)$	8	20.3	$\sigma = 73 \pm 4 \pm 5$ fb	$\sigma = 65 \pm 4$ fb (PowhegBox norm. to NNLO & gg2ZZ)	PLB 753, 552-572 (2016)
$\sigma^{fid}(ZZ^* \to 4\ell)$	7	4.6	$\sigma = 29.8 + 3.8 - 3.5 + 2.1 - 1.9$ fb	$\sigma = 25.6 + 1.3 - 1.1$ fb (PowhegBox & gg2ZZ)	JHEP 03, 128 (2013)
$\sigma^{fid}(ZZjj)$ EWK	13	139	$\sigma = 0.82 \pm 0.18 \pm 0.11$ fb	$\sigma = 0.61 \pm 0.03$ fb (Sherpa 2.2.2)	arXiv:2004.10612
Wjj EWK (m_{jj} > 500 GeV)	8	20.2	$\sigma = 159 \pm 10 \pm 26$ fb	$\sigma = 198 \pm 12$ fb (Powheg+Pythia8 NLO)	EPJC 77 (2017) 474
Wjj EWK (m_{jj} > 500 GeV)	7	4.7	$\sigma = 144 \pm 23 \pm 26$ fb	$\sigma = 144 \pm 11$ fb (Powheg+Pythia8 NLO)	EPJC 77 (2017) 474
Zjj EWK	13	139	$\sigma = 37.4 \pm 3.5 \pm 5.5$ fb	$\sigma = 39.5 \pm 3.6$ fb (Herwig7+VBFNLO)	EPJC 81 (2021) 163
Zjj EWK	8	20.3	$\sigma = 10.7 \pm 0.9 \pm 1.9$ fb	$\sigma = 9.38 + 0.3 - 0.4$ fb (PowhegBox (NLO))	JHEP 04, 031 (2014)

Figure 21: Table of used results. Uncertainties for the theoretical predictions are quoted from the original ATLAS papers.

Standard Model Production Cross Section Measurements II

ATLAS Preliminary

$\sqrt{s}$ = 5, 7, 8, 13 TeV

Status: February 2022

Model	E_{CM} [TeV]	$\int\mathcal{L}\,dt[fb^{-1}]$	Measurement	Theory	Reference
σ^{fid}(W) [n_{jet}=2, n_{b-jet}=1]	7	4.6	$\sigma = 2.2 \pm 0.2 \pm 0.5$ pb	$\sigma = 1.69 \pm 0.4$ pb (MCFM+D.P.I.)	JHEP 06, 084 (2013)
σ^{fid}(W) [n_{jet}=1, n_{b-jet}=1]	7	4.6	$\sigma = 5 \pm 0.5 \pm 1.2$ pb	$\sigma = 3.01 \pm 0.83$ pb (MCFM+D.P.I.)	JHEP 06, 084 (2013)
$\sigma^{fid}(W \to e\nu, \mu\nu)$	13	0.081	$\sigma = 8.03 \pm 0.01 \pm 0.23$ nb	$\sigma = 7.82 + 0.26 - 0.3$ nb (DYNNLO + CT14NNLO)	PLB 759 (2016) 601
$\sigma^{fid}(W \to e\nu, \mu\nu)$	8	20.2	$\sigma = 5247 \pm 0.6 \pm 111$ pb	$\sigma = 5120 \pm 142$ pb (DYNNLO + CT14NNLO)	EPJC 79 (2019) 760
$\sigma^{fid}(W \to e\nu, \mu\nu)$	7	4.6	$\sigma = 4.911 \pm 0.001 \pm 0.092$ nb	$\sigma = 4.777 + 0.12 - 0.14$ nb (DYNNLO + CT14NNLO)	EPJC 77 (2017) 367
$\sigma^{fid}(W \to e\nu, \mu\nu)$	5	0.025	$\sigma = 3.667 \pm 0.016 \pm 0.084$ nb	$\sigma = 3.58 \pm 0.11$ nb (DYNNLO + CT14NNLO)	EPJC 79 (2019) 128
$\sigma^{fid}(W,Z \to qq)$	7	4.6	$\sigma = 8.5 \pm 0.8 \pm 1.5$ pb	$\sigma = 5.1 \pm 0.5$ pb (MCFM)	NJP 16, 113013 (2014)
$\sigma^{fid}(Z \to bb)$	8	19.5	$\sigma = 2.02 \pm 0.2 \pm 0.26$ pb	$\sigma = 2.02 + 0.25 - 0.19$ pb (Powheg)	PLB 738, 25-43 (2014)
σ^{fid}(Z) [$n_{b-jet} \geq 2$]	13	35.6	$\sigma = 1.32 \pm 0.01 \pm 0.21$ pb	$\sigma = 1.16 + 0.22 - 0.15$ pb (Sherpa 2.2.1)	JHEP 07 (2020) 044
σ^{fid}(Z) [$n_{b-jet} \geq 2$]	7	4.6	$\sigma = 520 \pm 20 + 74 - 72$ fb	$\sigma = 410 \pm 61$ fb (MCFM)	JHEP 10, 141, (2014)
σ^{fid}(Z) [$n_{b-jet} \geq 1$]	13	35.6	$\sigma = 10.9 \pm 0.03 \pm 1.08$ pb	$\sigma = 10.15 + 0.32 - 0.82$ pb (Sherpa 2.2.1)	JHEP 07 (2020) 044
σ^{fid}(Z) [$n_{b-jet} \geq 1$]	7	4.6	$\sigma = 4820 \pm 60 + 360 - 380$ fb	$\sigma = 5230 + 691 - 711$ fb (MCFM)	JHEP 10, 141, (2014)
$\sigma^{fid}(Z \to \tau\tau)$	7	4.6	$\sigma = 1690 \pm 35 + 95 - 121$ fb	$\sigma = 1468.27 + 35.942 - 40.604$ fb (MC@NLO + HERAPDFNLO)	PRD 91, 052005 (2015)
$\sigma^{fid}(Z \to ee, \mu\mu)$	13	3.2	$\sigma = 776 \pm 1 \pm 18$ pb	$\sigma = 744 + 22 - 28$ pb (DYNNLO+CT14 NNLO)	JHEP 02 (2017) 117
$\sigma^{fid}(Z \to ee, \mu\mu)$	8	20.2	$\sigma = 506 \pm 0.2 \pm 11$ pb	$\sigma = 486 + 13.6 - 16$ pb (DYNNLO+CT14 NNLO)	JHEP 02 (2017) 117
$\sigma^{fid}(Z \to ee, \mu\mu)$	7	4.6	$\sigma = 451 \pm 0.4 \pm 8.8$ pb	$\sigma = 432 + 12.5 - 13.8$ pb (DYNNLO+CT14 NNLO)	JHEP 02 (2017) 117
$\sigma^{fid}(Z \to ee, \mu\mu)$	5	0.025	$\sigma = 374.5 \pm 3.4 \pm 7.9$ pb	$\sigma = 356 + 9 - 10$ pb (DYNNLO + CT14NNLO)	EPJC 79 (2019) 128
$t\bar{t}\gamma$	13	36.1	$\sigma = 521 \pm 9 \pm 41$ fb	$\sigma = 495 \pm 99$ fb (PRD 83 (2011) 074013)	EPJC 79 (2019) 382
$t\bar{t}\gamma$	8	20.2	$\sigma = 139 \pm 7 \pm 17$ fb	$\sigma = 151 \pm 25$ fb (MadGraph+PRD 83 (2011) 074013)	JHEP 11 (2017) 086
$t\bar{t}\gamma$	7	4.6	$\sigma = 63 \pm 8 + 17 - 13$ fb	$\sigma = 48 \pm 10$ fb (Whizard+NLO)	PRD 91, 072007 (2015)
$t\bar{t}W$	13	36.1	$\sigma = 870 \pm 130 \pm 140$ fb	$\sigma = 600 \pm 72$ fb (Madgraph5 + aMCNLO)	PRD 99, 072009 (2019)
$t\bar{t}W$	8	20.3	$\sigma = 369 + 86 - 79 \pm 44$ fb	$\sigma = 232 \pm 32$ fb (MCFM)	JHEP 11, 172 (2015)
$t\bar{t}Z$	13	139	$\sigma = 990 \pm 50 \pm 80$ fb	$\sigma = 840 \pm 90$ fb (Madgraph5 + aMCNLO)	Eur. Phys. J. C 81 (2021) 737
$t\bar{t}Z$	8	20.3	$\sigma = 176 + 52 - 48 \pm 24$ fb	$\sigma = 215 \pm 30$ fb (HELAC-NLO)	JHEP 11, 172 (2015)
$\sigma^{fid}(W \to e\nu, \mu\nu)/\sigma^{fid}(Z \to ee, \mu\mu)$ [$n_{jet} \geq 4$]	7	4.6	Ratio $= 7.62 \pm 0.19 \pm 0.94$	Ratio $= 8.87 \pm 0.16$ (Blackhat)	EPJC 74 (2014) 3168
$\sigma^{fid}(W \to e\nu, \mu\nu)/\sigma^{fid}(Z \to ee, \mu\mu)$ [$n_{jet} \geq 3$]	7	4.6	Ratio $= 8.18 \pm 0.08 \pm 0.51$	Ratio $= 8.97 \pm 0.1$ (Blackhat)	EPJC 74 (2014) 3168
$\sigma^{fid}(W \to e\nu, \mu\nu)/\sigma^{fid}(Z \to ee, \mu\mu)$ [$n_{jet} \geq 2$]	7	4.6	Ratio $= 8.64 \pm 0.04 \pm 0.32$	Ratio $= 8.789 \pm 0.046$ (Blackhat)	EPJC 74 (2014) 3168
$\sigma^{fid}(W \to e\nu, \mu\nu)/\sigma^{fid}(Z \to ee, \mu\mu)$ [$n_{jet} \geq 1$]	7	4.6	Ratio $= 8.54 \pm 0.02 \pm 0.25$	Ratio $= 8.676 \pm 0.031$ (Blackhat)	EPJC 74 (2014) 3168
$\sigma^{fid}(W \to e\nu, \mu\nu)/\sigma^{fid}(Z \to ee, \mu\mu)$	13	0.081	Ratio $= 10.31 \pm 0.04 \pm 0.2$	Ratio $= 10.54 \pm 0.12$ (DYNNLO + CT14NNLO)	PLB 759 (2016) 601
$\sigma^{fid}(W \to e\nu, \mu\nu)/\sigma^{fid}(Z \to ee, \mu\mu)$	7	4.6	Ratio $= 9.78 \pm 0.006 \pm 0.049$	Ratio $= 9.92 \pm 0.1$ (old)	EPJC 77 (2017) 367
W [njet $\geq$ 7]	8	20.2	$\sigma = 0.041 \pm 0.003 \pm 0.032$ pb	$\sigma = 0.052 + 0.007 - 0.02$ pb (Sherpa 2.2.1 NLO)	JHEP 05 (2018) 077
W [njet $\geq$ 7]	7	4.6	$\sigma = 0.041 \pm 0.0068 \pm 0.031$ pb		EPJC 75 (2015) 82
W [njet $\geq$ 6]	8	20.2	$\sigma = 0.22 \pm 0.006 \pm 0.121$ pb	$\sigma = 0.239 + 0.03 - 0.084$ pb (Sherpa 2.2.1 NLO)	JHEP 05 (2018) 077
W [njet $\geq$ 6]	7	4.6	$\sigma = 0.199 \pm 0.019 \pm 0.11$ pb		EPJC 75 (2015) 82
W [njet $\geq$ 5]	8	20.2	$\sigma = 1.107 \pm 0.013 \pm 0.423$ pb	$\sigma = 1.1 + 0.13 - 0.38$ pb (Sherpa 2.2.1 NLO)	JHEP 05 (2018) 077
W [njet $\geq$ 5]	7	4.6	$\sigma = 0.877 \pm 0.032 \pm 0.301$ pb	$\sigma = 0.933 \pm 0.027$ pb (Blackhat)	EPJC 75 (2015) 82
W [njet $\geq$ 4]	8	20.2	$\sigma = 5.47 \pm 0.03 \pm 1.47$ pb	$\sigma = 5 + 0.5 - 1.4$ pb (Sherpa 2.2.1 NLO)	JHEP 05 (2018) 077
W [njet $\geq$ 4]	7	4.6	$\sigma = 4.241 \pm 0.056 \pm 0.885$ pb	$\sigma = 4.67 \pm 0.06$ pb (Blackhat)	EPJC 75 (2015) 82
W [njet $\geq$ 3]	8	20.2	$\sigma = 26.38 \pm 0.06 \pm 5.34$ pb	$\sigma = 23.6 + 1.3 - 5$ pb (Sherpa 2.2.1 NLO)	JHEP 05 (2018) 077
W [njet $\geq$ 3]	7	4.6	$\sigma = 21.82 \pm 0.1 \pm 3.23$ pb	$\sigma = 23.47 \pm 0.22$ pb (Blackhat)	EPJC 75 (2015) 82
W [njet $\geq$ 2]	8	20.2	$\sigma = 128.35 \pm 0.12 \pm 20.39$ pb	$\sigma = 126.5 + 2.1 - 14.4$ pb (Sherpa 2.2.1 NLO)	JHEP 05 (2018) 077
W [njet $\geq$ 2]	7	4.6	$\sigma = 111.7 \pm 0.2 \pm 12.2$ pb	$\sigma = 111.98 \pm 0.44$ pb (Blackhat)	EPJC 75 (2015) 82
W [njet $\geq$ 1]	8	20.2	$\sigma = 564.71 \pm 0.24 \pm 72.13$ pb	$\sigma = 584 + 8 - 37$ pb (Sherpa 2.2.1 NLO)	JHEP 05 (2018) 077
W [njet $\geq$ 1]	7	4.6	$\sigma = 493.8 \pm 0.5 \pm 45.1$ pb	$\sigma = 474.22 \pm 0.84$ pb (Blackhat)	EPJC 75 (2015) 82
W	13	0.081	$\sigma = 190.1 \pm 0.2 \pm 6.4$ nb	$\sigma = 184.9 + 6 - 6.1$ nb (DYNNLO + CT14NNLO)	PLB 759 (2016) 601
W	8	20.2	$\sigma = 112.69 \pm 3.1$ nb	$\sigma = 110.919889503 \pm 3.7$ nb (DYNNLO + CT14NNLO)	EPJC 79 (2019) 760
W	7	4.6	$\sigma = 98.71 \pm 0.028 \pm 2.191$ nb	$\sigma = 95.9 \pm 2.9$ nb (DYNNLO + CT14NNLO)	EPJC 77 (2017) 367
Z [njet $\geq$ 7]	7	4.6	$\sigma = 0.0062 \pm 0.001456 \pm 0.00214$ pb		JHEP 07, 032 (2013)
Z [njet $\geq$ 6]	13	139	$\sigma = 0.000338 \pm 5.3e-05 \pm 5.5e-05$ pb	$\sigma = 0.000511 + 0.00034 - 0.00019$ pb (Sherpa (NLO QCD+ NLO EW corr))	ATLAS-CONF-2021-033
Z [njet $\geq$ 6]	7	4.6	$\sigma = 0.0253 \pm 0.00265 \pm 0.00595$ pb		JHEP 07, 032 (2013)
Z [njet = 5]	13	139	$\sigma = 0.0028 \pm 0.00015 \pm 0.00031$ pb	$\sigma = 0.00326 + 0.0022 - 0.0012$ pb (Sherpa (NLO QCD+ NLO EW corr))	ATLAS-CONF-2021-033
Z [njet $\geq$ 5]	7	4.6	$\sigma = 0.135 \pm 0.006 \pm 0.027$ pb		JHEP 07, 032 (2013)
Z [njet = 4]	13	139	$\sigma = 0.0227 \pm 0.00044 \pm 0.0023$ pb	$\sigma = 0.0234 + 0.015 - 0.0083$ pb (Sherpa (NLO QCD+ NLO EW corr))	ATLAS-CONF-2021-033
Z [njet $\geq$ 4]	7	4.6	$\sigma = 0.65 \pm 0.01 \pm 0.11$ pb	$\sigma = 0.646 \pm 0.031$ pb (Blackhat)	JHEP 07, 032 (2013)
Z [njet = 3]	13	139	$\sigma = 0.201 \pm 0.0014 \pm 0.015$ pb	$\sigma = 0.186 + 0.11 - 0.058$ pb (Sherpa (NLO QCD+ NLO EW corr))	ATLAS-CONF-2021-033
Z [njet $\geq$ 3]	7	4.6	$\sigma = 3.09 \pm 0.03 \pm 0.4$ pb	$\sigma = 3.1 \pm 0.14$ pb (Blackhat)	JHEP 07, 032 (2013)
Z [njet = 2]	13	139	$\sigma = 1.97 \pm 0.0039 \pm 0.098$ pb	$\sigma = 1.807 + 0.69 - 0.39$ pb (Sherpa (NLO QCD+ NLO EW corr))	ATLAS-CONF-2021-033
Z [njet $\geq$ 2]	7	4.6	$\sigma = 15.05 \pm 0.06 \pm 1.51$ pb	$\sigma = 14.9 \pm 0.4$ pb (Blackhat)	JHEP 07, 032 (2013)
Z [njet = 1]	13	139	$\sigma = 11.84 \pm 0.0081 \pm 0.57$ pb	$\sigma = 11.17 + 2.2 - 1.3$ pb (Sherpa (NLO QCD+ NLO EW corr))	ATLAS-CONF-2021-033
Z [njet $\geq$ 1]	7	4.6	$\sigma = 68.84 \pm 0.13 \pm 5.15$ pb	$\sigma = 64.8 \pm 3.1$ pb (Blackhat)	JHEP 07, 032 (2013)
Z	13	3.2	$\sigma = 58.43 \pm 0.03 \pm 1.66$ nb	$\sigma = 55.96 + 1.5 - 1.7$ nb (DYNNLO+CT14 NNLO)	JHEP 02 (2017) 117
Z	8	20.2	$\sigma = 34.24 \pm 0.03 \pm 0.92$ nb	$\sigma = 32.94 + 0.8 - 0.92$ nb (DYNNLO+CT14 NNLO)	JHEP 02 (2017) 117
Z	7	4.6	$\sigma = 29.53 \pm 0.03 \pm 0.77$ nb	$\sigma = 28.31 + 0.68 - 0.8$ nb (DYNNLO+CT14 NNLO)	JHEP 02 (2017) 117

Figure 22: Table of used results. Uncertainties for the theoretical predictions are quoted from the original ATLAS papers.

Standard Model Production Cross Section Measurements III

ATLAS Preliminary

$\sqrt{s}$ = 7, 8, 13 TeV

Status: February 2022

Model	E_{CM} [TeV]	$\int\mathcal{L}\,dt[fb^{-1}]$	Measurement	Theory	Reference
pp	8	50×10^{-8}	$\sigma = 96.07 \pm 0.18 \pm 0.91$ mb	$\sigma = 99.55 \pm 2.14$ mb (COMPETE HPR1R2)	PLB 761 (2016) 158
pp	7	8×10^{-8}	$\sigma = 95.35 \pm 0.38 \pm 1.3$ mb	$\sigma = 97.26 \pm 2.12$ mb (COMPETE HPR1R2)	Nucl. Phys. B, 486-548 (2014)
pp inelastic	13	6×10^{-8}	$\sigma = 79.3 \pm 2.9$ mb	$\sigma = 78.4 \pm 2$ mb (Schuler/Sjöstrand)	PRL 117, 182002 (2016)
pp inelastic	8	50×10^{-8}	$\sigma = 71.73 \pm 0.15 \pm 0.69$ mb	$\sigma = 73 \pm 2$ mb (Schuler/Sjöstrand)	PLB 761 (2016) 158
pp inelastic	7	8×10^{-8}	$\sigma = 71.34 \pm 0.36 \pm 0.83$ mb	$\sigma = 71.5 + 20 - 2$ mb (Schuler/Sjöstrand)	Nucl. Phys. B, 486-548 (2014)
$2.5 < y^* < 3.0$, $2 < m_{jj} < 5$ TeV	13	3.2	$\sigma = 850 \pm 53 + 68 - 91$ pb	$\sigma = 955 + 56 - 199$ pb (NLOJet++, CT14)	JHEP 05 (2018) 195
$2.5 < y^* < 3.0$, $2 < m_{jj} < 5$ TeV	7	4.5	$\sigma = 16 \pm 2 + 5.4 - 4.3$ pb	$\sigma = 18.4 + 2.2 - 4.3$ pb (NLOJet++, CT10)	JHEP 05, 059 (2014)
$2.0 < y^* < 2.5$, $1.3 < m_{jj} < 5$ TeV	13	3.2	$\sigma = 6.39 \pm 0.14 + 0.47 - 0.54$ nb	$\sigma = 6.7 + 0.5 - 1.3$ nb (NLOJet++, CT14)	JHEP 05 (2018) 195
$2.0 < y^* < 2.5$, $1.3 < m_{jj} < 5$ TeV	7	4.5	$\sigma = 371 \pm 9.7 + 81.5 - 72.1$ pb	$\sigma = 410.6 + 31 - 77.8$ pb (NLOJet++, CT10)	JHEP 05, 059 (2014)
$1.5 < y^* < 2.0$, $0.8 < m_{jj} < 4.6$ TeV	13	3.2	$\sigma = 16.13 \pm 0.17 \pm 1.09$ nb	$\sigma = 17.4 + 0.7 - 3.3$ nb (NLOJet++, CT14)	JHEP 05 (2018) 195
$1.5 < y^* < 2.0$, $0.8 < m_{jj} < 4.6$ TeV	7	4.5	$\sigma = 3.57 \pm 0.04 + 0.51 - 0.49$ nb	$\sigma = 3.7 + 0.21 - 0.62$ nb (NLOJet++, CT10)	JHEP 05, 059 (2014)
$1.0 < y^* < 1.5$, $0.5 < m_{jj} < 4.6$ TeV	13	3.2	$\sigma = 68.7 \pm 0.4 + 4 - 4.2$ nb	$\sigma = 68.5 + 7.7 - 10.3$ nb (NLOJet++, CT14)	JHEP 05 (2018) 195
$1.0 < y^* < 1.5$, $0.5 < m_{jj} < 4.6$ TeV	7	4.5	$\sigma = 10.12 \pm 0.07 + 1.02 - 1.03$ nb	$\sigma = 10.2 + 0.5 - 1.5$ nb (NLOJet++, CT10)	JHEP 05, 059 (2014)
$0.5 < y^* < 1.0$, $0.3 < m_{jj} < 4.3$ TeV	13	3.2	$\sigma = 117.6 \pm 0.5 + 6.8 - 6.9$ nb	$\sigma = 127.3 + 5.7 - 19$ nb (NLOJet++, CT14)	JHEP 05 (2018) 195
$0.5 < y^* < 1.0$, $0.3 < m_{jj} < 4.3$ TeV	7	4.5	$\sigma = 37.33 \pm 0.2 + 3.25 - 3.03$ nb	$\sigma = 37.3 + 1.6 - 5.1$ nb (NLOJet++, CT10)	JHEP 05, 059 (2014)
$y^* < 0.5$, $0.3 < m_{jj} < 4.3$ TeV	13	3.2	$\sigma = 111.2 \pm 0.4 + 6.2 - 6.3$ nb	$\sigma = 118.6 + 5.5 - 18.8$ nb (NLOJet++, CT14)	JHEP 05 (2018) 195
$y^* < 0.5$, $0.3 < m_{jj} < 4.3$ TeV	7	4.5	$\sigma = 35.47 \pm 0.15 + 2.79 - 2.66$ nb	$\sigma = 35.3 + 1.5 - 5.1$ nb (NLOJet++, CT10)	JHEP 05, 059 (2014)
Dijet R=0.4, $\lvert y\rvert < 3.0$, $y^* < 3.0$	13	3.2	$\sigma = 321 \pm 0.8 + 18.6 - 19$ nb	$\sigma = 340 + 17 - 54$ nb (NLOJet++, CT14)	JHEP 05 (2018) 195
Dijet R=0.4, $\lvert y\rvert < 3.0$, $y^* < 3.0$	7	4.5	$\sigma = 86.87 \pm 0.26 + 7.56 - 7.2$ nb	$\sigma = 86.9 + 4.7 - 12.4$ nb (NLOJet++, CT10)	JHEP 05, 059 (2014)
$2.5 < y^* < 3.0$, $2 < m_{jj} < 5$ TeV	7	4.5	$\sigma = 26.9 \pm 4.2 + 7.7 - 6.4$ pb	$\sigma = 23.5 + 2.7 - 2.8$ pb (NLOJet++, CT10)	JHEP 05, 059 (2014)
$2.0 < y^* < 2.5$, $1.3 < m_{jj} < 5$ TeV	7	4.5	$\sigma = 505 \pm 15.1 + 102.4 - 92.4$ pb	$\sigma = 526.9 + 37.5 - 46.3$ pb (NLOJet++, CT10)	JHEP 05, 059 (2014)
$1.5 < y^* < 2.0$, $0.8 < m_{jj} < 4.6$ TeV	7	4.5	$\sigma = 4.93 \pm 0.06 + 0.69 - 0.65$ nb	$\sigma = 4.78 + 0.23 - 0.34$ nb (NLOJet++, CT10)	JHEP 05, 059 (2014)
$1.0 < y^* < 1.5$, $0.5 < m_{jj} < 4.6$ TeV	7	4.5	$\sigma = 13.82 \pm 0.11 + 1.44 - 1.42$ nb	$\sigma = 13.2 + 0.5 - 0.8$ nb (NLOJet++, CT10)	JHEP 05, 059 (2014)
$0.5 < y^* < 1.0$, $0.3 < m_{jj} < 4.3$ TeV	7	4.5	$\sigma = 51.47 \pm 0.32 + 4.76 - 4.44$ nb	$\sigma = 48.7 + 1.3 - 2.5$ nb (NLOJet++, CT10)	JHEP 05, 059 (2014)
$y^* < 0.5$, $0.3 < m_{jj} < 4.3$ TeV	7	4.5	$\sigma = 48.21 \pm 0.23 + 4.03 - 3.8$ nb	$\sigma = 46.1 + 1.2 - 2.5$ nb (NLOJet++, CT10)	JHEP 05, 059 (2014)
Dijet R=0.6, $\lvert y\rvert < 3.0$, $y^* < 3.0$	7	4.5	$\sigma = 119 \pm 0.4 + 10.9 - 10.3$ nb	$\sigma = 113.3 + 3.1 - 6.1$ nb (NLOJet++, CT10)	JHEP 05, 059 (2014)
$2.5 < \lvert y\rvert < 3.0$, $p_T > 100$ GeV	13	3.2	$\sigma = 157 \pm 1 \pm 13$ nb	$\sigma = 165 + 13 - 18$ nb (NLOJet++, CT14)	JHEP 05 (2018) 195
$2.5 < \lvert y\rvert < 3.0$, $p_T > 100$ GeV	8	20.2	$\sigma = 45.3 \pm 0.3 + 3.9 - 3.8$ nb	$\sigma = 50.4 + 4.1 - 7.4$ nb (NLOJet++, CT14)	JHEP 09 (2017) 020
$2.5 < \lvert y\rvert < 3.0$, $p_T > 100$ GeV	7	4.5	$\sigma = 29.13 \pm 0.31 + 7.5 - 6.38$ nb	$\sigma = 32.6 + 2.1 - 3.2$ nb (NLOJet++, CT10)	JHEP 02, 153 (2015)
$2.0 < \lvert y\rvert < 2.5$, $p_T > 100$ GeV	13	3.2	$\sigma = 222 \pm 1 + 19 - 20$ nb	$\sigma = 241 + 19 - 26$ nb (NLOJet++, CT14)	JHEP 05 (2018) 195
$2.0 < \lvert y\rvert < 2.5$, $p_T > 100$ GeV	8	20.2	$\sigma = 79.8 \pm 0.4 \pm 5.4$ nb	$\sigma = 88.8 + 6.4 - 11.7$ nb (NLOJet++, CT14)	JHEP 09 (2017) 020
$2.0 < \lvert y\rvert < 2.5$, $p_T > 100$ GeV	7	4.5	$\sigma = 57.1 \pm 0.4 + 10.4 - 9.1$ nb	$\sigma = 60.7 + 3.3 - 5.1$ nb (NLOJet++, CT10)	JHEP 02, 153 (2015)
$1.5 < \lvert y\rvert < 2.0$, $p_T > 100$ GeV	13	3.2	$\sigma = 288 \pm 1 \pm 21$ nb	$\sigma = 317 + 24 - 33$ nb (NLOJet++, CT14)	JHEP 05 (2018) 195
$1.5 < \lvert y\rvert < 2.0$, $p_T > 100$ GeV	8	20.2	$\sigma = 111 \pm 0.4 + 6.9 - 6.8$ nb	$\sigma = 124.7 + 9.5 - 15.4$ nb (NLOJet++, CT14)	JHEP 09 (2017) 020
$1.5 < \lvert y\rvert < 2.0$, $p_T > 100$ GeV	7	4.5	$\sigma = 83.5 \pm 0.6 + 11.1 - 9.7$ nb	$\sigma = 88.3 + 4.7 - 7.1$ nb (NLOJet++, CT10)	JHEP 02, 153 (2015)
$1.0 < \lvert y\rvert < 1.5$, $p_T > 100$ GeV	13	3.2	$\sigma = 350 \pm 2 \pm 24$ nb	$\sigma = 383 + 28 - 38$ nb (NLOJet++, CT14)	JHEP 05 (2018) 195
$1.0 < \lvert y\rvert < 1.5$, $p_T > 100$ GeV	8	20.2	$\sigma = 145.4 \pm 0.5 + 8.9 - 8.6$ nb	$\sigma = 157 + 12 - 19$ nb (NLOJet++, CT14)	JHEP 09 (2017) 020
$1.0 < \lvert y\rvert < 1.5$, $p_T > 100$ GeV	7	4.5	$\sigma = 112.2 \pm 0.7 + 11 - 10.2$ nb	$\sigma = 113.1 + 5.8 - 9.2$ nb (NLOJet++, CT10)	JHEP 02, 153 (2015)
$0.5 < \lvert y\rvert < 1.0$, $p_T > 100$ GeV	13	3.2	$\sigma = 401 \pm 2 \pm 24$ nb	$\sigma = 431 + 33 - 44$ nb (NLOJet++, CT14)	JHEP 05 (2018) 195
$0.5 < \lvert y\rvert < 1.0$, $p_T > 100$ GeV	8	20.2	$\sigma = 167.9 \pm 0.5 + 9.6 - 9.4$ nb	$\sigma = 182 + 14 - 23$ nb (NLOJet++, CT14)	JHEP 09 (2017) 020
$0.5 < \lvert y\rvert < 1.0$, $p_T > 100$ GeV	7	4.5	$\sigma = 136.9 \pm 0.8 + 10.9 - 10.5$ nb	$\sigma = 132.3 + 6.9 - 10.7$ nb (NLOJet++, CT10)	JHEP 02, 153 (2015)
$\lvert y\rvert < 0.5$, $p_T > 100$ GeV	13	3.2	$\sigma = 427 \pm 2 \pm 24$ nb	$\sigma = 459 + 35 - 49$ nb (NLOJet++, CT14)	JHEP 05 (2018) 195
$\lvert y\rvert < 0.5$, $p_T > 100$ GeV	8	20.2	$\sigma = 177 \pm 0.5 + 9.6 - 9.4$ nb	$\sigma = 196 + 14 - 25$ nb (NLOJet++, CT14)	JHEP 09 (2017) 020
$\lvert y\rvert < 0.5$, $p_T > 100$ GeV	7	4.5	$\sigma = 145.1 \pm 0.8 + 10.7 - 10.6$ nb	$\sigma = 142.7 + 7.4 - 11.5$ nb (NLOJet++, CT10)	JHEP 02, 153 (2015)
Incl. jet R=0.4, $\lvert y\rvert < 3.0$	13	3.2	$\sigma = 1845 \pm 4 + 119 - 120$ nb	$\sigma = 1997 + 152 - 208$ nb (NLOJet++, CT14)	JHEP 05 (2018) 195
Incl. jet R=0.4, $\lvert y\rvert < 3.0$	8	20.2	$\sigma = 726.4 \pm 1.1 + 42.7 - 41.8$ nb	$\sigma = 800 + 59 - 100$ nb (NLOJet++, CT14)	JHEP 09 (2017) 020
Incl. jet R=0.4, $\lvert y\rvert < 3.0$	7	4.5	$\sigma = 563.9 \pm 1.5 + 55.4 - 51.4$ nb	$\sigma = 569.8 + 29.5 - 46.3$ nb (NLOJet++, CT10)	JHEP 02, 153 (2015)
$2.5 < \lvert y\rvert < 3.0$, $p_T > 100$ GeV	8	20.2	$\sigma = 58.6 \pm 0.8 + 5.8 - 5.6$ nb	$\sigma = 59.8 + 4.1 - 6.6$ nb (NLOJet++, CT14)	JHEP 09 (2017) 020
$2.5 < \lvert y\rvert < 3.0$, $p_T > 100$ GeV	7	4.5	$\sigma = 37.5 \pm 0.4 + 9.4 - 8.4$ nb	$\sigma = 36.9 + 3.7 - 2.4$ nb (NLOJet++, CT10)	JHEP 02, 153 (2015)
$2.0 < \lvert y\rvert < 2.5$, $p_T > 100$ GeV	8	20.2	$\sigma = 100.5 \pm 1.1 + 8.6 - 8.3$ nb	$\sigma = 105.8 + 6.6 - 11.4$ nb (NLOJet++, CT14)	JHEP 09 (2017) 020
$2.0 < \lvert y\rvert < 2.5$, $p_T > 100$ GeV	7	4.5	$\sigma = 69.7 \pm 0.6 + 13.5 - 12.7$ nb	$\sigma = 68.6 + 6.3 - 4.3$ nb (NLOJet++, CT10)	JHEP 02, 153 (2015)
$1.5 < \lvert y\rvert < 2.0$, $p_T > 100$ GeV	8	20.2	$\sigma = 140.3 \pm 1.2 + 11.1 - 10.8$ nb	$\sigma = 149.8 + 9.4 - 14.6$ nb (NLOJet++, CT14)	JHEP 09 (2017) 020
$1.5 < \lvert y\rvert < 2.0$, $p_T > 100$ GeV	7	4.5	$\sigma = 105.5 \pm 0.7 + 16 - 15.2$ nb	$\sigma = 100.2 + 9.2 - 5.9$ nb (NLOJet++, CT10)	JHEP 02, 153 (2015)
$1.0 < \lvert y\rvert < 1.5$, $p_T > 100$ GeV	8	20.2	$\sigma = 190.7 \pm 1.4 + 15 - 14.6$ nb	$\sigma = 189 + 11 - 18$ nb (NLOJet++, CT14)	JHEP 09 (2017) 020
$1.0 < \lvert y\rvert < 1.5$, $p_T > 100$ GeV	7	4.5	$\sigma = 139.8 \pm 0.9 + 16.5 - 16.2$ nb	$\sigma = 128.8 + 11.7 - 7.4$ nb (NLOJet++, CT10)	JHEP 02, 153 (2015)
$0.5 < \lvert y\rvert < 1.0$, $p_T > 100$ GeV	8	20.2	$\sigma = 221.6 \pm 1.5 + 16.5 - 15.8$ nb	$\sigma = 220 + 13 - 21$ nb (NLOJet++, CT14)	JHEP 09 (2017) 020
$0.5 < \lvert y\rvert < 1.0$, $p_T > 100$ GeV	7	4.5	$\sigma = 172.7 \pm 0.9 + 15.9 - 14.3$ nb	$\sigma = 151 + 13.8 - 8.6$ nb (NLOJet++, CT10)	JHEP 02, 153 (2015)
$\lvert y\rvert < 0.5$, $p_T > 100$ GeV	8	20.2	$\sigma = 239.3 \pm 1.6 + 16.5 - 15.9$ nb	$\sigma = 237 + 14 - 24$ nb (NLOJet++, CT14)	JHEP 09 (2017) 020
$\lvert y\rvert < 0.5$, $p_T > 100$ GeV	7	4.5	$\sigma = 187 \pm 0.9 + 15.1 - 15$ nb	$\sigma = 162.9 + 15 - 9.2$ nb (NLOJet++, CT10)	JHEP 02, 153 (2015)
Incl. jet R=0.6, $\lvert y\rvert < 3.0$	8	20.2	$\sigma = 951 \pm 3 + 72 - 70$ nb	$\sigma = 961 + 58 - 95$ nb (NLOJet++, CT14)	JHEP 09 (2017) 020
Incl. jet R=0.6, $\lvert y\rvert < 3.0$	7	4.5	$\sigma = 712.3 \pm 1.9 + 79.9 - 76$ nb	$\sigma = 648.3 + 58.96 - 37.1$ nb (NLOJet++, CT10)	JHEP 02, 153 (2015)

Figure 23: Table of used results. Uncertainties for the theoretical predictions are quoted from the original ATLAS papers.

Standard Model Production Cross Section Measurements IV

Status: February 2022

ATLAS Preliminary

$\sqrt{s}$ = 5, 7, 8, 13 TeV

Model	E_{CM} [TeV]	$\int\mathcal{L}\,dt[fb^{-1}]$	Measurement	Theory	Reference
$\sigma^{fid}(W\gamma\gamma \to \ell\nu\gamma\gamma)[n_{jet}=0]$	8	20.3	$\sigma = 2.9 + 0.8 - 0.7 + 1 - 0.9$ fb	$\sigma = 1.88 \pm 0.2$ fb (MCFM NLO)	PRL 115, 031802 (2015)
$\sigma^{fid}(W\gamma\gamma \to \ell\nu\gamma\gamma)$	8	20.3	$\sigma = 6.1 + 1.1 - 1 \pm 1.2$ fb	$\sigma = 2.9 \pm 0.16$ fb (MCFM NLO)	PRL 115, 031802 (2015)
$\sigma^{fid}(Z\gamma\gamma \to \ell\ell\gamma\gamma)[n_{jet}=0]$	8	20.3	$\sigma = 3.48 + 0.61 - 0.56 + 0.3 - 0.26$ fb	$\sigma = 2.91 + 0.23 - 0.12$ fb (MCFM NLO)	PRD 93, 112002 (2016)
$\sigma^{fid}(Z\gamma\gamma \to \ell\ell\gamma\gamma)$	8	20.3	$\sigma = 5.07 + 0.73 - 0.68 + 0.42 - 0.39$ fb	$\sigma = 3.7 + 0.21 - 0.11$ fb (MCFM NLO)	PRD 93, 112002 (2016)
$\sigma^{fid}(WW\gamma \to e\nu\mu\nu\gamma)$	8	20.2	$\sigma = 1.5 \pm 0.9 \pm 0.5$ fb	$\sigma = 2 \pm 0.1$ fb (VBFNLO+CT14 (NLO))	EPJC 77 (2017) 646
$\sigma^{fid}(Z\gamma \to \ell\ell\gamma)[n_{jet} = 0]$	8	20.3	$\sigma = 1.189 \pm 0.009 + 0.073 - 0.067$ pb	$\sigma = 1.23 + 0.01 - 0.018$ pb (NNLO)	PRD 93, 112002 (2016)
$\sigma^{fid}(Z\gamma \to \ell\ell\gamma)[n_{jet} = 0]$	7	4.6	$\sigma = 1.05 \pm 0.02 \pm 0.11$ pb	$\sigma = 1.107 + 0.012 - 0.018$ pb (NNLO)	PRD 87, 112003 (2013)
$\sigma^{fid}(Z\gamma \to \nu\nu\gamma)$	13	36.1	$\sigma = 83.7 + 3.6 - 3.5 + 7.1 - 6.5$ fb	$\sigma = 78.1 \pm 4.7$ fb (MCFM (NNLO))	JHEP 12 (2018) 010
$\sigma^{fid}(Z\gamma \to \nu\nu\gamma)$	8	20.3	$\sigma = 68 \pm 4 + 33 - 32$ fb	$\sigma = 81.4 + 2.4 - 2.2$ fb (NNLO)	PRD 93, 112002 (2016)
$\sigma^{fid}(Z\gamma \to \nu\nu\gamma)$	7	4.6	$\sigma = 0.133 \pm 0.013 \pm 0.021$ pb	$\sigma = 0.156 \pm 0.012$ pb (MCFM NLO)	PRD 87, 112003 (2013)
$\sigma^{fid}(Z\gamma \to \ell\ell\gamma)$	13	36.1	$\sigma = 533.7 \pm 2.1 \pm 15.4$ fb	$\sigma = 515 + 20 - 19$ fb (Matrix NNLO QCD + NLO EW)	JHEP 03 (2020) 054
$\sigma^{fid}(Z\gamma \to \ell\ell\gamma)$	8	20.3	$\sigma = 1.507 \pm 0.01 + 0.083 - 0.078$ pb	$\sigma = 1.483 + 0.019 - 0.037$ pb (NNLO)	PRD 93, 112002 (2016), arXiv:1407.1618
$\sigma^{fid}(Z\gamma \to \ell\ell\gamma)$	7	4.6	$\sigma = 1.31 \pm 0.02 \pm 0.12$ pb	$\sigma = 1.327 + 0.026 - 0.037$ pb (NNLO)	PRD 87, 112003 (2013), arXiv:1407.1618
$Z\gamma jjEW$	13	139	$\sigma = 4.49 \pm 0.4 \pm 0.42$ fb	$\sigma = 4.73 \pm 0.52$ fb (Madgraph5 + aMCNLO)	ATLAS-CONF-2021-038
$Z\gamma jjEW$	8	20.3	$\sigma = 1.1 \pm 0.5 \pm 0.4$ fb	$\sigma = 0.94 \pm 0.09$ fb (VBFNLO)	JHEP 07 (2017) 107
$\sigma^{fid}(W\gamma \to \ell\nu\gamma)[n_{jet} = 0]$	7	4.6	$\sigma = 1.76 \pm 0.03 \pm 0.22$ pb	$\sigma = 1.674 + 0.056 - 0.064$ pb (NNLO)	PRD 87, 112003 (2013)
$\sigma^{fid}(W\gamma \to \ell\nu\gamma)$	7	4.6	$\sigma = 2.77 \pm 0.03 \pm 0.36$ pb	$\sigma = 2.658 \pm 0.11$ pb (NNLO)	PRD 87, 112003 (2013), arXiv:1407.1618
$\sigma^{fid}(\gamma\gamma)[\Delta R_{\gamma\gamma} > 0.4]$	13	139	$\sigma = 31.4 \pm 0.1 \pm 2.4$ pb	$\sigma = 29.7 + 2.4 - 2$ pb (NNLOjet (NNLO))	JHEP 11 (2021) 169
$\sigma^{fid}(\gamma\gamma)[\Delta R_{\gamma\gamma} > 0.4]$	8	20.2	$\sigma = 16.82 \pm 0.07 + 0.75 - 0.78$ pb	$\sigma = 14.2 + 1.25 - 0.91$ pb (2γNNLO + CT10)	PRD 95 (2017) 112005
$\sigma^{fid}(\gamma\gamma)[\Delta R_{\gamma\gamma} > 0.4]$	7	4.9	$\sigma = 44 + 3.2 - 4.2$ pb	$\sigma = 44 \pm 6$ pb (2γNNLO)	JHEP 01, 086 (2013)
γ	13	3.2	$\sigma = 399 \pm 0.4 \pm 16$ pb	$\sigma = 352 + 36 - 30$ pb (JETPHOX+MMHT2014 (NLO))	PLB 2017 04 072
γ	8	20.2	$\sigma = 56.8 \pm 0.1 + 5.8 - 5.6$ nb	$\sigma = 52.2 \pm 7$ nb (PETER (NLO+N^3LL))	JHEP 06 (2016) 005
γ	7	4.6	$\sigma = 359 \pm 3 + 22 - 16$ pb	$\sigma = 308 \pm 40$ pb (JETPHOX (NLO))	PRD 89, 052004 (2014)
$\sigma^{fid}(\gamma$+X) [1.52< $\lvert\eta^\gamma\rvert$ < 2.37]	8	20.2	$\sigma = 21 \pm 0.05 + 2.14 - 2.04$ nb	$\sigma = 16.6 \pm 3.3$ nb (JETPHOX (NLO))	JHEP 06 (2016) 005
$\sigma^{fid}(\gamma$+X) [1.52< $\lvert\eta^\gamma\rvert$ < 2.37]	7	4.6	$\sigma = 123 \pm 1 + 9 - 7$ pb	$\sigma = 105 \pm 15$ pb (JETPHOX (NLO))	PRD 89, 052004 (2014)
$\sigma^{fid}(\gamma$+X) [1.56< $\lvert\eta^\gamma\rvert$ < 1.81]	8	20.2	$\sigma = 6.7 \pm 0.02 \pm 0.71$ nb	$\sigma = 5.7 \pm 0.7$ nb (PETER (NLO+N^3LL))	JHEP 06 (2016) 005
$\sigma^{fid}(\gamma$+X) [1.81< $\lvert\eta^\gamma\rvert$ < 2.37]	8	20.2	$\sigma = 14.3 \pm 0.03 + 1.43 - 1.33$ nb	$\sigma = 12.7 \pm 1.8$ nb (PETER (NLO+N^3LL))	JHEP 06 (2016) 005
$\sigma^{fid}(\gamma$+X) [$\lvert\eta^\gamma\rvert$ <1.37]	8	20.2	$\sigma = 35.8 \pm 0.05 + 3.7 - 3.6$ nb	$\sigma = 33.8 \pm 4.5$ nb (PETER (NLO+N^3LL))	JHEP 06 (2016) 005
$\sigma^{fid}(\gamma$+X) [$\lvert\eta^\gamma\rvert$ <1.37]	7	4.6	$\sigma = 236 \pm 2 + 13 - 9$ pb	$\sigma = 203 \pm 25$ pb (JETPHOX (NLO))	PRD 89, 052004 (2014)
$\sigma^{fid}(\gamma$+X) [$\lvert\eta^\gamma\rvert$ <0.6]	8	20.2	$\sigma = 15.6 \pm 0.02 \pm 1.43$ nb	$\sigma = 14.8 \pm 2$ nb (PETER (NLO+N^3LL))	JHEP 06 (2016) 005
$\sigma^{fid}(\gamma$+X) [0.6< $\lvert\eta^\gamma\rvert$ < 1.37]	8	20.2	$\sigma = 20.2 \pm 0.03 + 2.24 - 2.14$ nb	$\sigma = 19 \pm 2.5$ nb (PETER (NLO+N^3LL))	JHEP 06 (2016) 005
γ [njet ≥ 1]	13	3.2	$\sigma = 300 \pm 0.4 \pm 12$ pb	$\sigma = 319 + 55 - 46$ pb (SHERPA (NLO))	PLB 780 (2018) 578
γ [njet ≥ 1]	8	20.2	$\sigma = 134 \pm 0.1 \pm 4$ pb	$\sigma = 128 + 11 - 9$ pb (JETPHOX (NLO))	Nucl. Phys. B, 918 (2017) 257
γ [njet ≥ 2]	8	20.2	$\sigma = 30.4 \pm 0.04 \pm 1.8$ pb	$\sigma = 29.2 + 2.8 - 2.7$ pb (NLOBlackhat+CT10)	Nucl. Phys. B, 918 (2017) 257
γ [njet ≥ 3]	8	20.2	$\sigma = 8.7 \pm 0.02 \pm 0.8$ pb	$\sigma = 9.5 + 0.9 - 1.2$ pb (NLOBlackhat+CT10)	Nucl. Phys. B, 918 (2017) 257
$t\bar{t}$	13	36.1	$\sigma = 826.4 \pm 3.6 \pm 19.6$ pb	$\sigma = 832 + 40 - 45$ pb (top++ NNLO+NNLL)	EPJC 80 (2020) 528
$t\bar{t}$	8	20.2	$\sigma = 242.9 \pm 1.7 \pm 8.6$ pb	$\sigma = 252.9 + 13.3 - 14.5$ pb (top++ NNLO+NNLL)	EPJC 74 (2014) 3109
$t\bar{t}$	7	4.6	$\sigma = 182.9 \pm 3.1 \pm 6.4$ pb	$\sigma = 177 + 10 - 11$ pb (top++ NNLO+NNLL)	EPJC 74 (2014) 3109
$t\bar{t}$	5	0.3	$\sigma = 66 \pm 4.5 \pm 1.6$ pb	$\sigma = 68.2 + 5.2 - 5.3$ pb (NNLO+NNLL QCD)	ATLAS-CONF-2021-003
$t\bar{t}t\bar{t}$	13	139	$\sigma = 24 \pm 4 \pm 5$ fb	$\sigma = 12 \pm 2.4$ fb (NLO QCD + EW)	JHEP 11 (2021) 118
$t\bar{t}$ $[n_{jet} = 3]$	7	4.7	$\sigma = 4.34 \pm 0.06 \pm 0.64$ pb		JHEP 01, 020 (2015)
$t\bar{t}$ $[n_{jet} = 4]$	7	4.7	$\sigma = 3.76 \pm 0.05 \pm 0.27$ pb		JHEP 01, 020 (2015)
$t\bar{t}$ $[n_{jet} = 5]$	7	4.7	$\sigma = 1.72 \pm 0.04 \pm 0.16$ pb		JHEP 01, 020 (2015)
$t\bar{t}$ $[n_{jet} = 6]$	7	4.7	$\sigma = 0.611 \pm 0.024 \pm 0.083$ pb		JHEP 01, 020 (2015)
$t\bar{t}$ $[n_{jet} = 7]$	7	4.7	$\sigma = 0.161 \pm 0.007 \pm 0.033$ pb		JHEP 01, 020 (2015)
$t\bar{t}$ $[n_{jet} \geq 8]$	7	4.7	$\sigma = 0.0425 \pm 0.004 \pm 0.012$ pb		JHEP 01, 020 (2015)
tZj	13	139	$\sigma = 97 \pm 13 \pm 7$ fb	$\sigma = 102 + 5 - 2$ fb (Madgraph5 + aMCNLO (NLO))	JHEP 07 (2020) 124
Wt	13	3.2	$\sigma = 94 \pm 10 + 28 - 23$ pb	$\sigma = 71.7 \pm 3.9$ pb (NLO+NNLL)	JHEP 01 (2018) 63
Wt	8	20.3	$\sigma = 23 \pm 1.3 + 3.4 - 3.7$ pb	$\sigma = 22.4 \pm 1.5$ pb (NLO+NLL)	JHEP 01, 064 (2016)
Wt	7	2.0	$\sigma = 16.8 \pm 2.9 \pm 3.9$ pb	$\sigma = 15.7 \pm 1.1$ pb (NLO+NLL)	PLB 716, 142-159 (2012)
t_{t-chan}	13	3.2	$\sigma = 247 \pm 6 \pm 46$ pb	$\sigma = 217 \pm 10$ pb (NLO+NLL)	JHEP 04 (2017) 086
t_{t-chan}	8	20.3	$\sigma = 89.6 \pm 1.7 + 7.2 - 6.4$ pb	$\sigma = 87.8 + 3.4 - 1.9$ pb (NLO+NLL)	EPJC 77 (2017) 531
t_{t-chan}	7	4.6	$\sigma = 68 \pm 2 \pm 8$ pb	$\sigma = 64.6 + 2.7 - 2$ pb (NLO+NLL)	PRD 90, 112006 (2014)
t_{s-chan}	8	20.3	$\sigma = 4.8 \pm 0.8 + 1.6 - 1.3$ pb	$\sigma = 5.61 \pm 0.22$ pb (NLO+NNL)	LB 756, 228-246 (2016)

Figure 24: Table of used results. Uncertainties for the theoretical predictions are quoted from the original ATLAS papers.

10 Cross-section measurements as a function of centre-of-mass energy $\sqrt{s}$

Summary of total production cross-section measurements by ATLAS presented as a function of centre-of-mass energy from 7 to 13 TeV for a few selected processes. The diboson measurements are scaled by a factor 0.1 to allow a presentation without overlaps.

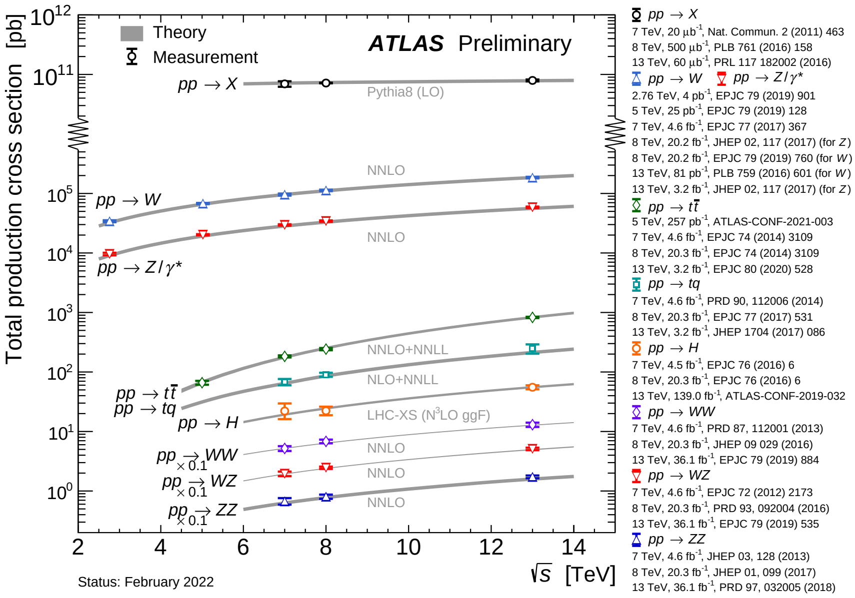

Figure 25: Summary of total production cross-section measurements by ATLAS presented as a function of centre-of-mass energy from 2.76 to 13 TeV for a few selected processes. Note: Figure do not have any hyperlinks. Since this plot is made with pure ROOT macros, we need to take a different approach. We can try to add this in next round.

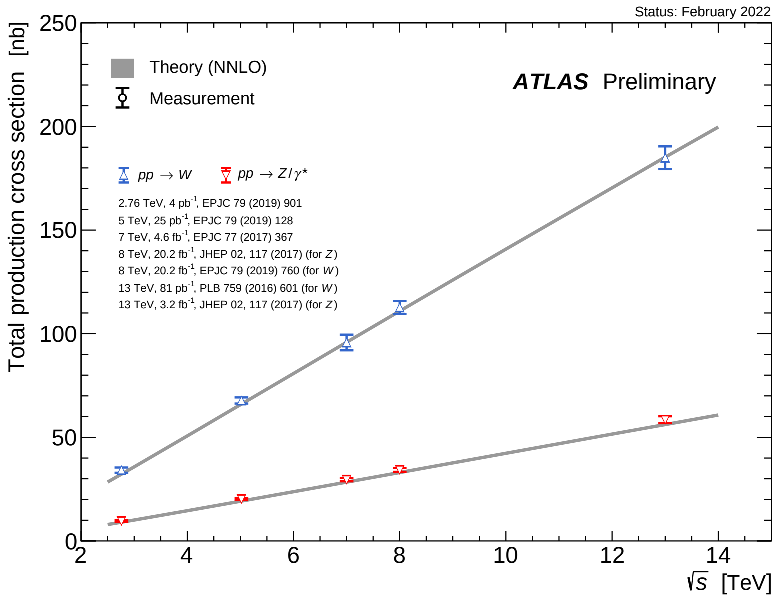

Figure 26: Summary of total production cross-section measurements of electro-weak gauge boson by ATLAS presented as a function of centre-of-mass energy from 2.76 to 13 TeV. Note: Figure do not have any hyperlinks. Since this plot is made with pure ROOT macros, we need to take a different approach. We can try to add this in next round.

References

[1] ATLAS Collaboration, *Gitlab page for Summary plots*, (2020),
URL: https://gitlab.cern.ch/atlas-physics/sm/StandardModelTools_SummaryPlots/SummaryPlots (cit. on p. 2).

[2] ATLAS Collaboration, *Standard Model Summary Plots July 2021*, (2021), URL: https://atlas.web.cern.ch/Atlas/GROUPS/PHYSICS/PUBNOTES/ATL-PHYS-PUB-2021-032/ (cit. on p. 2).

[3] ATLAS Collaboration,
Observation of WWW Production in pp Collisions at $\sqrt{s}$=13 TeV with the ATLAS Detector,
tech. rep. arXiv:2201.13045[hep-ex], 2022, URL: https://arxiv.org/pdf/2201.13045.pdf (cit. on p. 2).

[4] ATLAS Collaboration, *Combined measurement of the total and differential cross sections in the $H \to \gamma\gamma$ and the $H \to ZZ^* \to 4\ell$ decay channels at $\sqrt{s}$ =13 TeV with the ATLAS detector*,
tech. rep. ATLAS-CONF-2022-002, CERN, 2022, URL: https://atlas.web.cern.ch/Atlas/GROUPS/PHYSICS/CONFNOTES/ATLAS-CONF-2022-002/ (cit. on p. 2).

[5] ATLAS Collaboration, *Measurements of the Higgs boson production in the $H \to \tau^+\tau^-$ decay channel in $p\,p$ collisions at 13TeV with the ATLAS detector*, tech. rep., 2022,
URL: https://arxiv.org/pdf/2201.08269.pdf (cit. on p. 2).

[6] ATLAS Collaboration, *Combined measurements of Higgs boson production and decay using up to 139 fb^{-1} of proton-proton collision data at $\sqrt{s}$ =13 TeV collected with the ATLAS experiment*,
tech. rep. ATLAS-CONF-2022-002, CERN, 2021, URL: https://atlas.web.cern.ch/Atlas/GROUPS/PHYSICS/CONFNOTES/ATLAS-CONF-2021-053/ (cit. on p. 2).